Marine Mammal Science

Abundance and temporal trends of fin whales in the Eastern Midriff Islands Region, Gulf of California, Mexico

Journal:	*Marine Mammal Science*
Manuscript ID	MMSCI-5686.R2
Wiley - Manuscript type:	Article (Direct Via EEO)
Date Submitted by the Author:	17-Jun-2025
Complete List of Authors:	Arredondo-Sáinz, Joel A.; Centro de Investigación Científica y de Educación Superior de Ensenada, Conservation Biology Department Pérez-Puig, Héctor; Prescott College, Marine Mamal Program. Prescott College Kino Bay Center for Cultural and Ecological Studies Pardo, Mario; Centro de Investigación Científica y de Educación Superior de Ensenada, Unidad La Paz Heckel, Gisela; Centro de Investigacion Cientifica y de Educacion Superior de Ensenada, Conservation Biology Department
Keywords:	abundance estimation, Balaenoptera physalus, Bayesian time series, mark-recapture, population dynamics

Abundance and temporal trends of fin whales in the Eastern Midriff Islands Region, Gulf of California, Mexico

Joel A. Arredondo-Sáinz[1], Héctor Pérez-Puig[2], Mario A. Pardo[3], Gisela Heckel[1,*]

[1] Centro de Investigación Científica y de Educación Superior de Ensenada (CICESE), Departamento de Biología de la Conservación, Ensenada, Baja California, Mexico

[2] Marine Mammal Program, Prescott College Kino Bay Center for Cultural and Ecological Studies, Bahía de Kino, Sonora, Mexico.

[3] Secretaría de Ciencia, Humanidades, Tecnología e Innovación (SECIHTI) - CICESE-Unidad Académica La Paz, Laboratorio de Macroecología Marina. La Paz, Baja California Sur, Mexico.

***Correspondence**

Gisela Heckel, Carretera Ensenada-Tijuana 3918, Zona Playitas, 22860 Ensenada, Baja California, Mexico.

Email: gheckel@cicese.mx

Abstract

The fin whales (*Balaenoptera physalus*) in the Gulf of California comprise a resident population genetically isolated from the rest of the North Pacific. The species occurs seasonally in the biologically productive Eastern Midriff Islands Region (EMIR), located between 28.4°N and 29.4°N and 111.9°W and 112.8°W in the central portion of the Gulf of California, in which the present study estimated fin whale abundance using photo-identification data collected via weekly small-boat surveys conducted from 2009 to 2017. In total, 1,082 fin whales were recorded in 454 sightings, during 287 surveys that totaled 1,924 hr of research effort. After a photo comparison process that used photographs from both sides of the dorsal fin, 376 unique individuals were identified. Only 180 capture histories were used for mark-recapture analysis. A mark ratio of 0.48 was obtained which was used to inflate the abundance estimates. A Jolly-Seber/POPAN mark-recapture model, incorporating a transience effect on apparent survival, yielded a superpopulation size of $\hat{N}$ = 462 (SE_{Un} = 41.45, 95%CI [381 – 543]). The estimates for the years 2010-2016 were fairly constant, from 211 (95% CI [126-293]) to 313 (95% CI [232-395]), with confidence intervals having substantial overlap. A CJS model with two classes was used to estimate probability of survival, with the "transient" class having a $\phi_t = 0.68\ (\mathrm{SE} = 0.061, 95\%\mathrm{CI}\ [0.55 – 0.78])$, and individuals seen multiple times a $\phi_m = 0.915\ (\mathrm{SE} = 0.034, 95\%\ \mathrm{CI}[0.82 – 0.96])$. A hierarchical Bayesian time series analysis of encounter rates collected from 2012 to 2017 showed evidence of seasonality, with whales mostly present during the cold season (December-May), which coincides with the local upwelling regime. This information adds to the value of the EMIR as an important area for fin whale conservation in the Gulf of California.

KEYWORDS

abundance estimation, *Balaenoptera physalus,* Bayesian time series, mark-recapture, population dynamics

1 | INTRODUCTION

Fin whales (*Balaenoptera physalus* Linnaeus, 1758) are a Mysticete species with a worldwide distribution and occuring in all major oceans, mostly at temperate and polar latitudes (Jefferson et al., 2015). In the eastern North Pacific, a small, resident, and genetically-isolated population occurs in the Gulf of California (Bérubé et al., 2002; Rivera-León et al., 2019; Tershy et al., 1993; Urbán-Ramírez et al., 2005), having been founded approximately 9,000 years ago (Pérez-Álvarez et al., 2021). This population, as well as all fin whales and other cetaceans in Mexican waters, are protected by Mexican federal law (NOM-059-SEMARNAT-2010; SEMARNAT, 2019).

The Gulf of California is a marginal sea in the eastern Pacific Ocean, located between the Baja California Peninsula and mainland Mexico (20°-32°N and 105.5°-114.5°W, Fig. 1) (Espinosa-Carreón & Valdez-Holguín, 2007), with an approximate length of 1,400 km and an area of 259,000 km^2 (Álvarez-Borrego & Lara-Lara, 1991). The sea floor depth ranges from 200 m in the north to more than 3,600 m in the south (Lluch-Cota et al., 2007). The gulf contains more than 900 islands, with the largest in the Midriff Islands Region to its north (Álvarez-Borrego & Lara-Lara, 1991), which has a variety of underwater ridges, channels, and landforms. The strong and stable water column mixing observed in the region is influenced mainly by upwelling and tidal regimes, which result in high primary productivity (Álvarez-Borrego, 2010), creating a habitat on which rely several species of sea birds (Anderson et al., 2017) and marine mammals (Urbán-Ramírez et al., 2005). Four seasons have been defined in the Gulf of California, based on meteorological and oceanographic processes related to upwelling and primary productivity. Two relatively brief transition periods (November and June) separate the warm season, occurring from July to October, from the cold season, occurring from December to May (Álvarez-Borrego & Lara-Lara, 1991; Burgos-Othón, 2018; Hidalgo-González & Álvarez-Borrego, 2001).

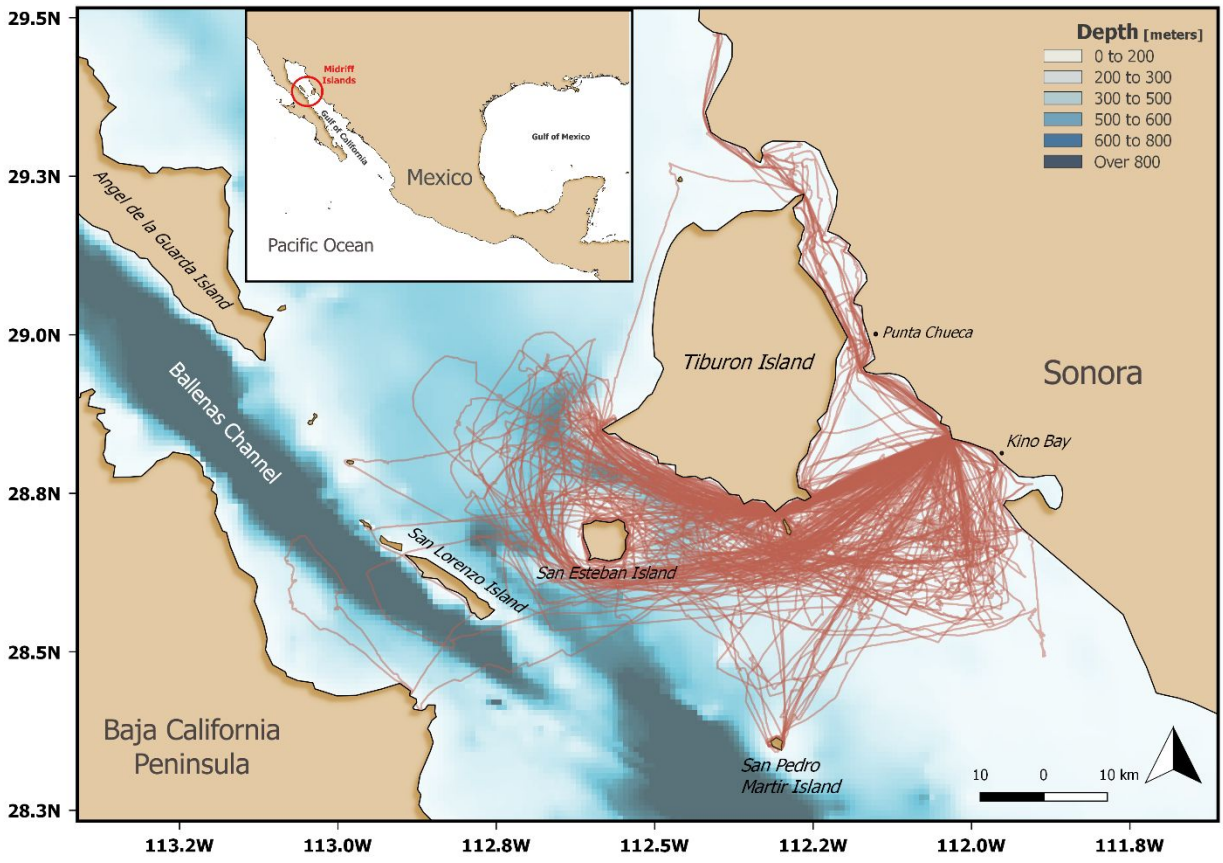

FIGURE 1 Study area in the Eastern Midriff Islands Region (EMIR) in the Gulf of California, Mexico. The GPS tracks in red represent the surveys undertaken from 2012 to 2017.

Fin whales occur throughout the Gulf of California, with their movements there seeming not to follow a regular or predictable pattern (Urbán-Ramírez et al., 2005). Some satellite-tagged animals (n = 8) were observed to spend the cold season in the southwestern gulf (Loreto-La Paz corridor) and the waters between Santa Rosalía and the southern Midriff Islands Region, moving northward along the gulf's western margin. During the warm season, these individuals moved within the central gulf and did not reach the eastern margin, located south of the Midriff Islands Region (Jiménez-López et al., 2019).

However, fin whales are also known to occur along the gulf's eastern coast (Enríquez-Paredes, 1996; Martínez-Villalba, 2008).

According to the International Union for Conservation of Nature (IUCN), the abundance of fin whales worldwide is thought to be around 100,000 individuals (Cooke, 2018), although no current population estimates are specifically available for the North Pacific. The last assessment of the North Pacific western stock, accepted by the International Whaling Commission Scientific Committee, and conducted in the 1970s, estimated the number at 17,000 individuals (Allen, 1977; Ohsumi & Wada, 1974). Published estimates of fin whale abundance for the Gulf of California vary from the 291 individuals photo-identified for solely the Ballenas Channel for 1983 to 1986 (Tershy et al., 1990) to the 829 (95% CI [594-3,229]) estimated for the entire gulf for 1986 to 1990 (Gerrodette & Palacios, 1996).

Most research effort conducted on the species has focused on the western and southwestern gulf (Díaz-Guzmán, 2006; Enríquez-Paredes, 1996; Montesinos-Laffont, 2016) as well as the Ballenas Channel (Ladrón-De-Guevara et al., 2015; Tershy et al., 1990), whereas only a few sightings have been reported for the eastern coast (Martínez-Villalba, 2008), for which there is no description of seasonal variation. The previous abundance estimates have remained in unpublished theses (Díaz-Guzmán, 2006; Enríquez-Paredes, 1996; Montesinos-Laffont, 2016), while long-term abundance monitoring is required to document the increase or decrease in a population, as in this species protected by Mexican law. In addition, there are significant threats to the conservation of this species in the Gulf of California, such as the risk of collision with large ships or changes in the habitat caused by climate change. Therefore, we aimed both to estimate species abundance as well as survival rates in the Eastern Midriff Islands Region (EMIR) (28.4°N- 29.4°N and 111.9°W- 112.8°W), using photographic mark-recapture techniques, and to quantify temporal trends for the species, using data collected during weekly surveys conducted from 2009 to 2017.

2 | MATERIALS AND METHODS

2.1 | Data collection and processing

Our main study area was the Eastern Midriff Islands Region (EMIR), which is characterized by coastal upwelling during the cold season. From December 2009 to November 2017, we carried out 287 surveys, on a weekly basis, in an area limited by the Sonora coast to the east, San Esteban Island to the west, Tiburon Island to the north, and San Pedro Martir Island to the south (Fig. 1). Surveys were conducted on a 7-m length boat with a 115-HP outboard engine. The search effort totaled 1,924 hr, of which 1,012 hr was carried out during the cold season, 239 hr during the cold-warm transition season, 492 hr during the warm season, and 181 hr during the warm-cold transition season (Fig. 2 - see detailed table S1, in Supporting Information). The mean search effort time per survey was 6.7 hr, with surveys conducted only in good sea conditions, that is, a maximum 3 in Beaufort scale. Taking into account the aforementioned seasons, we considered that a year in our study began in the December of one year and ended in the November of the next. To test for effort homogeneity year-on-year, we performed a non-parametric Kruskal-Wallis test on the hours navigated per day, as this variable did not present a normal distribution (Shapiro-Wilk test, W=0.967, n = 287, p < 0.001). The aim of these surveys was to record and photograph as many fin whales as possible; therefore, the navigation routes followed were not pre-established, although we did try to cover the entire study area throughout each month. At least two observers searched continuously for fin whales with 7x50 hand-held binoculars, covering the area 180 degrees in front of the vessel. During each sighting, we recorded the number of whales and their apparent behavior. We took photographs of individual whales with a Canon EOS 7D camera fitted with a Canon lens (70-300 mm, f/4-5.6 IS USM), focusing on the dorsal fin and the pigmentation of its surrounding area. While we prioritized taking digital photographs of the whale's right side, both sides

were photographed when possible. We photographed fin whales on 89% of the surveys (effort was calculated with all surveys).

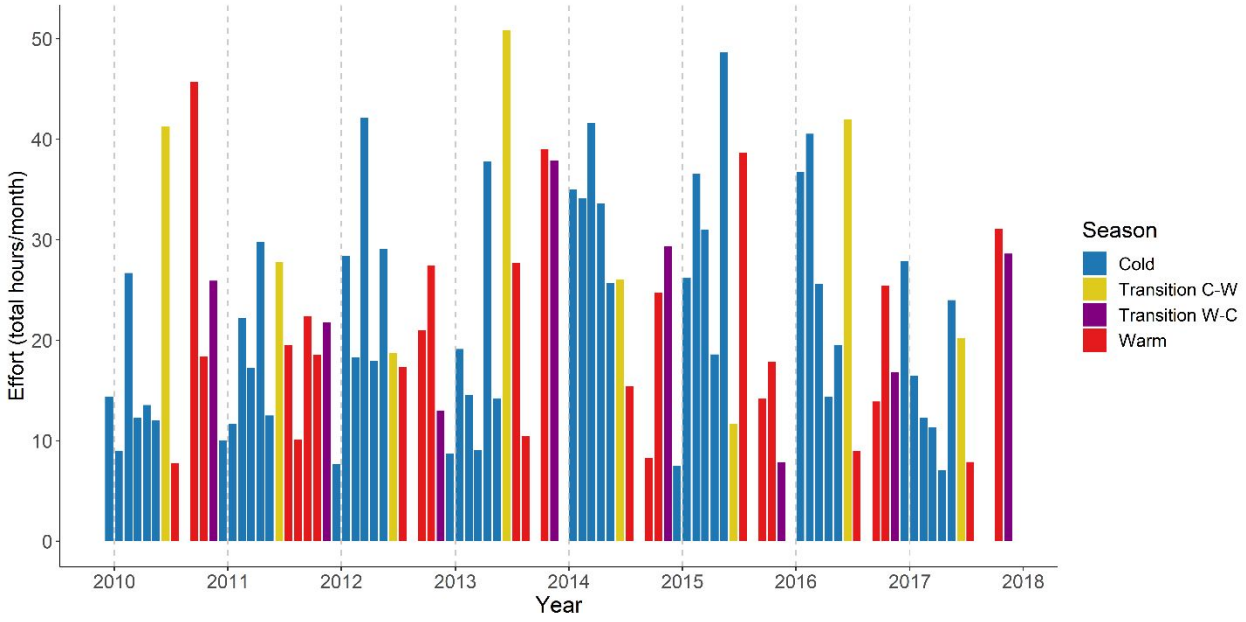

FIGURE 2 Search effort hours per month during the eight years comprising the present study (2009-2017). The data are colored depending on the seasons surveyed. Transition C-W = Transition from cold to warm season; Transition W-C = Transition from warm to cold season.

Two independent experienced observers organized and compared photographs using the ACDSee Photo Studio Professional 2021 program (Version 14.0). After each survey, we kept only the best photograph per individual per sighting, selected based on optimal focus, contrast, light, parallel angle, and clear visibility of the dorsal fin. In total, 1,243 photo-identification photographs were kept, predominantly of the right side of the dorsal fin. Photographs were visually compared across the photo-database to identify potential recaptures of individuals across different sightings. Calves were excluded from this

process and from subsequent mark-recapture analyses (Schleimer et al., 2019). Although the common protocol for fin whale photo-identification recommends two separate photographs per individual—one of the dorsal fin and another of the chevron/blaze (Agler et al., 1990), we found that reliable recaptures could be established using a single photograph that included both the natural marks (shape, nicks, scars) and distinguishable skin pigmentation on the dorsal fin.

Photo-identifications were graded regarding quality and distinctiveness following the protocol of the Sarasota Dolphin Research Group (Friday et al., 2000; Sarasota Dolphin Research Program, 2005; Urian et al., 2014). Quality takes into account focus/clarity, contrast, angle, partial and proportion of the frame filled by the fin. The sum of these characteristics gave each photo an overall quality score with three levels, with Q1 meaning excellent quality and Q3 meaning poor quality. A description of the score values used for photo quality is in Supplementary Information 2. "Distinctiveness" refers to how some whales are easier to mark as recapture due to their physical characteristics (shape, nicks, scars, and pigmentation) following Agler et al. (1990) (Supplementary Information 3). We gave each photo a distinctiveness rating from 1 to 3, with D1 meaning very distinctive, D2 medium level with one or two distinctive features on the dorsal fin, and D3 meaning not distinctive (Sarasota Dolphin Research Program, 2005). Based on this quality and distinctiveness classification, we only kept individuals with photo qualities Q1 and Q2 and distinctiveness D1 and D2.

Photo comparisons were first conducted within the same year, followed by a year-to-year paired comparison. For each year, the best photograph per differentiated individual was selected to build an annual catalog, which was then cross-referenced year-to-year to establish recaptures. The comparison process of the right and left sides was analyzed separately. However, using detailed field notes that documented side-specific encounters, we linked right- and left-side identifications to the same individual when morphological features were aligned. A final step involved comparing the right-side inter-annual catalog with "unique lefts"—left-side photographs with no associated right-side match—to resolve

additional recaptured individuals. In all cases, a match was confirmed only when at least two trained observers reached consensus. Based on these photo-identification results, we compiled a comprehensive catalog and constructed (encounter) recapture histories for each individual to support mark-recapture analysis.

A rate of discovery curve was constructed showing the number of new individuals added to our catalog related to the number of total photo-identifications analyzed. It is important to note that this includes intra-yearly photo-identifications. After a comparison in each year only one photo passed to the inter-yearly comparison which is why the total number of photographs in the catalog is less than shown in this graph (Fig. 4). As can be observed the graph begins to curve down, indicating an increasing number of recaptures (Darling & Morowitz, 1986). Another observation is that some years had considerably less photo-identifications collected, even though the survey effort was the same.

2.2 | Estimation of survival and abundance

The issue of reliable identification can bias abundance estimates. After removing the individuals with the lowest photo quality (Q3) and distinctiveness score (D3), we obtained the encounter histories for 180 individuals. We used these for mark-recapture analysis to estimate abundance and survival.

We carried out a goodness-of-fit (GOF) test on the fully parameterized Cormack-Jolly-Seber (CJS) model using the *R2Ucare* package (Gimenez et al., 2018). To adjust for extra-binomial variation we obtained an overdispersion factor (Burnham & Anderson, 2002; Lebreton et al., 1992) from the R2UCare CJS GOF test ratio: $\hat{c} = \frac{X^2}{df}$. We used the Jolly-Seber open capture-recapture model to estimate abundance and the Cormack-Jolly-Seber model (CJS) to estimate survival using RMark (Laake, 2013) and MARK v10.1 (White & Burnham, 1999). Transience was addressed with a time varying indicator for where an individual was in its first survival interval, which was adjusted for this study after the work of Schleimer

et al. (2018) in R. Transience was codified as a binary time design variable, not a usual covariate, since it was derived from the capture histories. It resembles a design variable, and is a string of digits with a 1 marking the sampling period where an individual was seen for the first time.

We used the Jolly-Seber model (Jolly, 1965; Seber, 1965) in its POPAN parameterization (Schwarz & Arnason, 1996) to obtain yearly abundances as well as the superpopulation size. The superpopulation consists of all individuals present in the study area between 2009 and 2017. The Jolly-Seber model is an open capture-recapture model that permits births and deaths, as well as immigration and emigration. Most of the model's key assumptions are similar to the CJS model but with the addition of assumptions about unmarked individuals. It assumes the following: 1) The probability of capture for marked and unmarked animals is the same for each occasion; 2) All animals have the same apparent survival probability; 3) Marked animals do not lose their markings; 4) The duration of one capture occasion is negligible compared with the duration of the subsequent sampling occasions; and 5) Individuals observed on each occasion are a random sample of the population visiting the region (Amstrup et al., 2005; Jolly, 1965; Schwarz & Arnason, 1996; Seber, 1965).

We adjusted the Akaike Information Criterion (AIC) (Akaike, 1985; Burnham & Anderson, 2002), taking into account the small sample size and the overdispersion parameter $\hat{c}$. Model ranking was based on $QAIC_c$ (Quasi-Akaike Information Criterion). We carried out model averaging for derived parameters as well as the real parameters ϕ and p, in MARK. The contribution of each model to the average parameter results presented is proportional to its corresponding $QAIC_c$ weight and was calculated automatically by MARK. For POPAN we kept survival constant (.), varied it by time (*time*), used a temporal linear trend (Time), considered the transient effect (lower apparent survival for individuals seen only once), an additive effect (~trans+time) influencing the parameter independently, and an interaction term (~trans:time). Capture probability and probability of entry were modeled as constant, time dependent or with a temporal linear trend. Population size was kept constant.

Furthermore, we estimated a mark ratio (based on Urian et al., 2015):

$$MR = \frac{n_m}{n_t}$$

Where n_m represents the marked individuals selected with photo qualities Q1 and Q2, and distinctiveness D1 and D2, and n_t is the total number of individuals in the catalog. The mark ratio was used in the total estimated abundance:

$$\hat{N}_{total} = \frac{\hat{N}_m}{MR}$$

Where $\hat{N}_m$ is the estimated abundance from marked individuals selected and *MR* is the mark ratio.

The CJS models were developed with two classes to obtain separate estimates for survival and recapture probability in MARK. In the present study, we used the *a2* notation to differentiate the classes "transients" for individuals seen only once, and the rest, individuals seen multiple times, for which me used the subscript "m" for multiple recaptures. For both parameters we tried time dependence per class or fixing the parameter as constant. For both cases only the top models, the ones that contained relevant information measured as fit through QDeviance or the lowest QAICc, were used to estimate survival.

2.3 | Time series analysis

To ascertain temporal variations in the fin whale population in the EMIR, we analyzed the whale counts obtained (observed whales), relative to the survey effort in hours, as a function of time, in order to identify possible signals, such as the long-term trend, the seasonal pattern, and the interannual variations from 2010 to 2017. We stated these signals as the fixed and random effects in a Bayesian regression analysis conducted on several alternative models, using the integrated nested Laplace

approximation (INLA; Rue et al., 2009) in R (R Core Team, 2023). The graphs were created using the *ggplot2* package (Wickham et al., 2022), while the *dplyr* package was used for data organization, along with the rest of the *tidyverse* (Wickham et al., 2019). Both to avoid the noise generated by counts conducted on a weekly basis and given that the seasonal scale was the highest frequency we aimed to identify, the first step was to estimate one-month running means for the counts and the survey effort in hours, in order to estimate the encounter rates. The INLA time series analysis undertaken followed the methods described by Gómez-Rubio (2020) and Ravishanker et al. (2023). The long-term trend was evaluated as a fixed effect of the continuous Julian day with up to three different alternative polynomial degrees. The seasonal pattern was stated as a cyclical random-walk effect based on the bimester of the year, as INLA requires that all the sample units for this type of random effect are represented in the data. The longitudinal nature of the data, and, therefore, its temporal autocorrelation was acknowledged in the model by introducing an autoregressive random effect on the bimester count (i.e., Julian bimester), corresponding to orders 1 or 2. Finally, the interannual signal was estimated as an autoregressive random effect of the year count, with different alternative orders of up to four. We used a Gaussian likelihood for the logarithmic transformation of the encounter rates as the response variable. In total, 20 alternative models were tested, with the best model chosen based on the lowest Watanabe-Akaike Information Criterion (WAIC). The mean predictive integral transform (PIT) and the Bayesian R-squared were also estimated for each model, as indices of fit and model accuracy, respectively. Some of these models included all of the four effects described, while others included only some of them. The complete structures of the best ten candidate models are presented in the *Results* section (Table 7), sorted into ascending WAIC.

3 | RESULTS

Between 2009 and 2017, we recorded 1,082 fin whales in 454 sightings, with no statistically significant differences found in effort among the years studied (Kruskal-Wallis test, H = 7.46, p = 0.38). We observed surface lunge feeding in 9.7% of all sightings. Over the eight years for which the study was conducted, the process of comparing and matching photographs resulted in the identification of 376 unique individuals in the region, based on photos taken of both sides of the dorsal fin. The final inter-yearly comparison process comprised 892 photo-identifications, from both sides of the dorsal fin (Fig. 3). Our catalog had 559 photo-identifications, with only the best photo from each side for each of the 376 individuals (if available). After the removal of individuals with Q3 and D3 we kept 180 individuals for capture-recapture analysis. Therefore, the mark ratio was 0.48. The fin type distribution of differentiated individuals is reported in Table 1.

TABLE 1. Fin type distribution for the Eastern Midriff Islands Region catalog. Total number of photo-identifications in the catalog was 559, with maximum two photos per individual (both sides of the dorsal fin). Total number of individuals in the catalog was 376. See Supporting Information 3 for fin type description.

Fin type	In catalog	%	No. with nicks	No. with scars	No. without nicks or scars
A	144	38.3	77	140	7
B	13	3.5	8	12	0
C	44	11.7	8	41	3
D	85	22.6	35	84	1
E	67	17.8	31	61	5
F	1	0.3	1	0	0
O	22	5.8	18	21	0

FIGURE 3 Photo-identification recaptures for individual 121 - both left and right side of the dorsal fin. In this case, the scar midway up the dorsum helped to confirm the photo-identification recaptures of this individual.

Notably, most photo-identifications and sightings occurred in the years 2009-2010 and 2013-2015 (Fig. 4). A large proportion of the individuals (60.7%; *n* = 224) were sighted only once in the study area, which coincides with the transience observed during the GOF testing. The highest number of photo-identifications (145) occurred during the year 2013-2014. The year with the lowest number of photo-identifications was 2011-2012, with 39. The year with the highest number of recaptures was 2013-2014,

with 46 (Table 2), indicating, at halfway through the course of the study, an increase in the discovery curve (Fig. 4). The lowest number of recaptures (4) was observed in 2016-2017, the last year in which the study was conducted. The rate of discovery of new individuals to the catalog decreased after 2012, which indicates that recaptures increased in percentage after this time (Fig. 4).

TABLE 2 m-*reduced matrix*¸ resulting from the integration of the information pertaining to both sides of the dorsal fin into one catalog, detailing the information contained in the fin whale capture histories for the present study. *i,j* = years; *R(i)* = individuals observed; *m(i,j)* = individuals observed during *i* that were first recaptured during *j*; *r(i)* = recaptures in *i*; and *m(j)* = recaptures in *j*.

Year (*i*)	*R(i)*	*m(i,j)*							*r(i)*
		2010-2011	2011-2012	2012-2013	2013-2014	2014-2015	2015-2016	2016-2017	
2009-2010	81	17	5	7	9	4	4	0	46
2010-2011	41		9	5	9	2	1	0	26
2011-2012	27			6	12	4	0	0	22
2012-2013	23				16	1	0	0	17
2013-2014	85					31	8	3	42
2014-2015	58						29	1	30
2015-2016	43							0	0
m(j)		17	14	18	46	42	42	4	

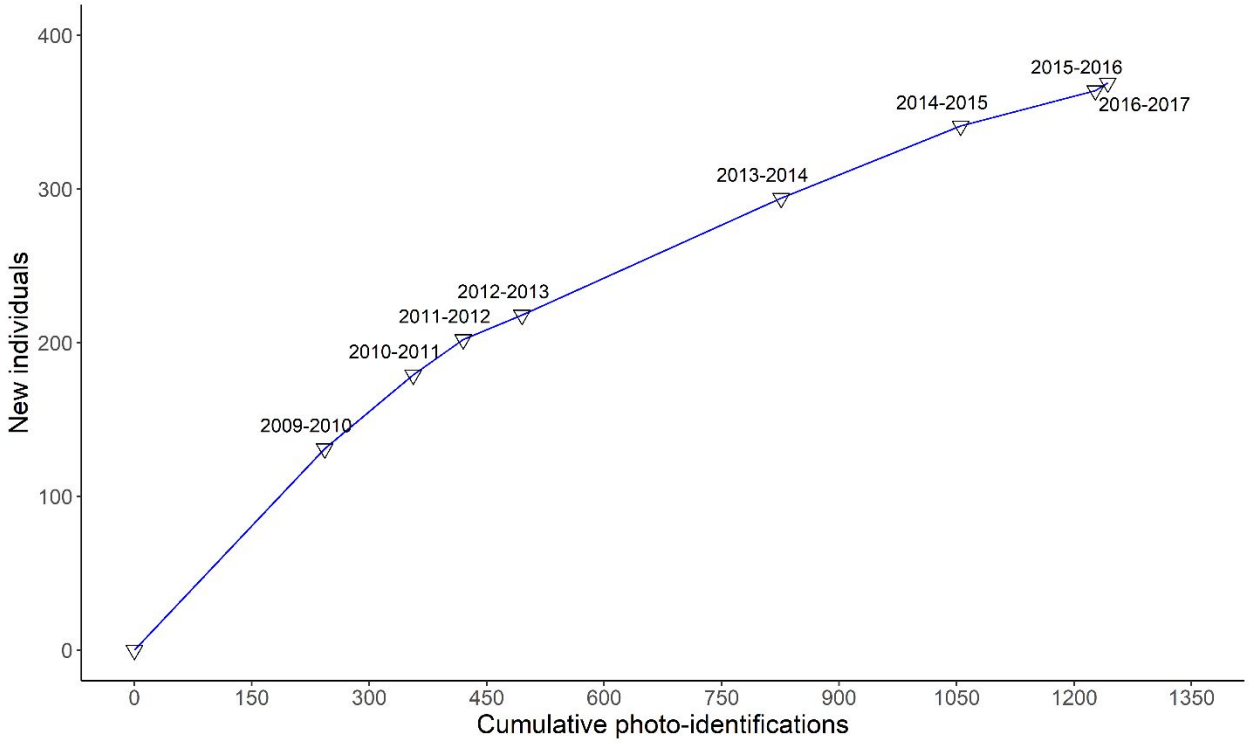

FIGURE 4 Rate of discovery of new individuals in the photo catalog, related to the number of photo-identifications analyzed. The total number of photoidentifications used from both sides of the dorsal fin for all individuals in this study, including intra-yearly recaptures.

3.1 | Abundance estimation

After the removal of individuals that did not have sufficient quality and distinctiveness in the catalog, we kept 180 capture histories, from the original 376 individuals. This means that the mark ratio for our study was $MR = \frac{180}{376} = 0.479$.

The summary information for the 180 capture histories used for estimating abundance is shown as an *m*-reduced matrix (Table 2)**.** The CJS R2UCare GOF test results showed that the CJS model fit the data $\left(X^2_{OVERALL} = 25.802, df = 22, p = 0.26\right)$. Neither the tests for evidence of trap-dependence (TEST2.CT) nor transience (TEST.3Sr) showed statistical evidence for a lack of fit (Table 3). Closer inspection of the

297 subcomponents for TEST3.Sr had only one year with a statistically significant deviation (2015-2016, Table
298 3). Even though there was no evidence for systematic transience during GOF testing, addressing it
299 improved the QDeviance and QAICc in the models that incorporated it. The estimated overdispersion
300 correction factor obtained was $\hat{c} = 1.172818$ which was used for model selection and variance inflation
301 both for the CJS and POPAN models, since separate GOF tests are unavailable for POPAN.

302

303 **TABLE 3** Goodness-of-fit test results for the Cormack-Jolly-Seber model per subcomponent. TEST2.CT
304 checks for trap dependence. The transient subcomponent 3.SR is shown per year. The only statistically
305 significant *p*-value is highlighted in bold.

Test	Component	χ^2	*df*	*p-value*
General	TEST2.CT	9.71	5	0.084
General	TEST2.CL	2.865	6	0.826
General	TEST3.Sm	3.58	6	0.734
General	TEST3.Sr	9.65	5	0.086
3.Sr Sub C.	2011-2012	0.644	1	0.422
3.Sr Sub C.	2012-2013	0.345	1	0.557
3.Sr Sub C.	2013-2014	0.313	1	0.576
3.Sr Sub C.	2014-2015	2.028	1	0.154
3.Sr Sub C.	2015-2016	6.320	1	**0.012***
3.Sr Sub C.	2016-2017	0	0	0

306

307 The best POPAN model was $\phi_{(trans:Time)}p_{(time)}pent_{(time)}N_{(.)}$ according to the QAIC$_c$ weights (Table 4), it
308 was also the one that best supported the data according to its QDeviance, which was the lowest in the
309 model table**.** Only the models that had a relevant measure of QAIC$_c$ are included, even though more
310 models were run. Note that the parameter count reported is different than what is expected
311 theoretically due to aliasing, meaning that MARK could not estimate it due to model structure

312 constraints, identifiability issues or redundancy or sparse data. The values presented are as reported
313 from RMark, to avoid penalizing models where parameters were not estimated properly. It was apparent
314 from observing the beta and real estimates that there were estimation problems for some of them,
315 which is why the number reported may differ from what is theoretically expected. Model averaging was
316 done in MARK, which uses the QAICc weights to determine the contribution of each model to the
317 averaged value.

318

319 **TABLE 4** Jolly-Seber POPAN models, descriptive statistics, and $QAIC_c$ support for model selection.
320 Parameters: ϕ = survival probability; p = capture probability; *pent* = entry probability; and *N*= abundance
321 estimate. A dot in parentheses (.) indicates that the parameter is constant for all occasions, while (*time*)
322 indicates time dependence, corresponding to a different parameter value for each occasion, (*T*) indicates
323 a temporal linear trend.

Rank	Model	Parameters	$QAIC_c$	$\Delta QAIC_c$	$QAIC_c$ weight	QDeviance
I	$\phi_{(trans:Time)}p_{(time)}pent_{(time)}N_{(.)}$	15	734.41	0	0.27272	703.0262
II	$\phi_{(trans)}p_{(time)}pent_{(time)}N_{(.)}$	15	734.81	0.4053	0.2227	703.4314
III	$\phi_{(trans+Time)}p_{(time)}pent_{(time)}N_{(.)}$	16	735.88	1.4679	0.13091	702.3051
IV	$\phi_{(trans)}p_{(time)}pent_{(T)}N_{(.)}$	13	736.96	2.5482	0.07628	709.9148
V	$\phi_{(trans:Time)}p_{(time)}pent_{(.)}N_{(.)}$	12	737.00	2.5944	0.07453	712.1125
VI	$\phi_{(trans:Time)}p_{(time)}pent_{(T)}N_{(.)}$	13	737.05	2.6419	0.07279	710.0084
VII	$\phi_{(trans)}p_{(time)}pent_{(.)}N_{(.)}$	12	737.05	2.6438	0.07272	712.1619
VII	$\phi_{(trans+Time)}p_{(time)}pent_{(Time)}N_{(.)}$	14	738.26	3.8515	0.03975	709.0541
VIII	$\phi_{(trans+Time)}p_{(time)}pent_{(.)}N_{(.)}$	13	738.37	3.9627	0.0376	711.3292

324

325 The model-averaged superpopulation estimate was $\hat{N}$ = 222 (unconditional SE = 19.9, 95%CI [183 – 261]),
326 the percentage of variation attributable to model variation was 22.16 %. After inflating with the mark

ratio (*MR=0.48*) the superpopulation estimate was $\hat{N}$ = 462 (SE_{Un} = 41.45, 95% CI [381 – 543). The estimates for the years 2010-2016 were fairly constant, from 211 (95% CI [126-293]) to 313 (95% CI [232-395]), with confidence intervals having substantial overlap (Table 5).

TABLE 5 Jolly-Seber POPAN model averaged annual abundance estimates, inflated with the mark ratio (*MR=0.48*). Unconditional standard error, which considers model selection uncertainty. The last column is the percentage of variation due to model differences in model averaging.

Year	Abundance	SE_{Un}	Lower 95% CL	Upper 95% CL	%variation MS
2010-2011	313	41.65	232	395	32.61%
2011-2012	284	36.39	213	366	39.71%
2012-2013	256	40.30	177	338	56.88%
2013-2014	276	30.09	217	357	20.48%
2014-2015	242	34.38	175	324	37.20%
2015-2016	211	43.29	126	293	42.72%

3.2 | Estimates of survival

The top ranked model was $\phi_{(a2-./.)}p_{(t)}$ with a QAICc weight of 0.93 and a QDeviance = 106.4 (Table 6). Overall, the two-class structure ("transients" and individuals seen multiple times, see Methods for definitions) for survival yielded a good fit, especially for more parsimonious models with less complexity. A model with time dependence in both parameters without the two-class approach yielded a good fit as well but was not ranked as high due to its higher parameter count (Model III). The two-class structure was also used for recapture probability but the models that incorporated it did not rank as high (Table 6).

342 The survival estimate for the transient class in the top-ranked model was $\phi_t = 0.68$ (SE = 0.061, 95% CI
343 [0.55– 0.78]), while the multiple recaptures class had a $\phi_m = 0.915$ (SE = 0.034, 95% CI [0.819– 0.962]).

344

345 **TABLE 6** Cormack-Jolly-Seber models with descriptive statistics ranked by QAICc. The *a2* notation
346 separates the parameter of survival for the first time an individual whale was sighted from the
347 parameter for whales seen multiple times.

Rank	Model	#par	$QAIC_c$	$\Delta QAIC_c$	Weight	QDeviance
I	$\phi_{(a2-./.)}p_{(t)}$	9	688.8398	0	0.93337	106.4257
II	$\phi_{(a2-./t)}p_{(t)}$	14	696.1809	7.3411	0.02377	103.0596
III	$\phi_{(t)}p_{(t)}$	13	696.4583	7.6185	0.02069	105.5033
IV	$\phi_{(a2-./.)}p_{(a2-t/t)}$	15	697.4073	8.5675	0.01287	102.107
V	$\phi_{(a2-t/.)}p_{(t)}$	15	698.3168	9.477	0.00817	103.0165
VI	$\phi_{(a2-t/t)}p_{(t)}$	19	702.2541	13.4143	0.00114	98.1088

348

349 The survival probability estimates were lower for the transient class than for the “multiple recaptures”
350 class as expected, which reflects the fact that transients likely emigrated permanently from the study
351 area. Although model averaged estimates were explored, they were not informative due to the large
352 influence of the top model QAICc weight. In the POPAN models developed, the model-averaged survival
353 estimates for the intermediate years were distributed between 0.827 to 0.881 with a lower 95% CL of
354 0.638 and an upper 95% CL of 0.951, which are similar to the values obtained from CJS.

The probability of recapture is reported for the top CJS model as well (Table 7). Even though the two-class strategy was used for recapture probability, those models did not rank well in our results. The time dependent *p* in the top-ranked model had values between 0.12 and 0.78 in their 95% CIs. All the means obtained were above 0.2, which is relevant in connection with the bias due to the time length of each sampling period in comparison to the time between successive sampling events (Table 7).

TABLE 7. Probability of recapture obtained from the top- ranked CJS model. Estimates are not shown for the first or last sampling periods because they are unreliable.

Year	*p*	SE	Lower 95% CL	Upper 95% CL
2011	0.31	0.07	0.19	0.46
2012	0.21	0.06	0.12	0.34
2013	0.25	0.06	0.16	0.37
2014	0.66	0.07	0.51	0.78
2015	0.48	0.07	0.35	0.61
2016	0.46	0.07	0.33	0.60

3.3 |Time series analysis

The number of fin whales sighted per survey ranged from 0 to 39, with most surveys sighting no individuals (Fig. 5). The group with the most frequent sightings comprised two individuals, while we observed only twelve calves throughout the study period.

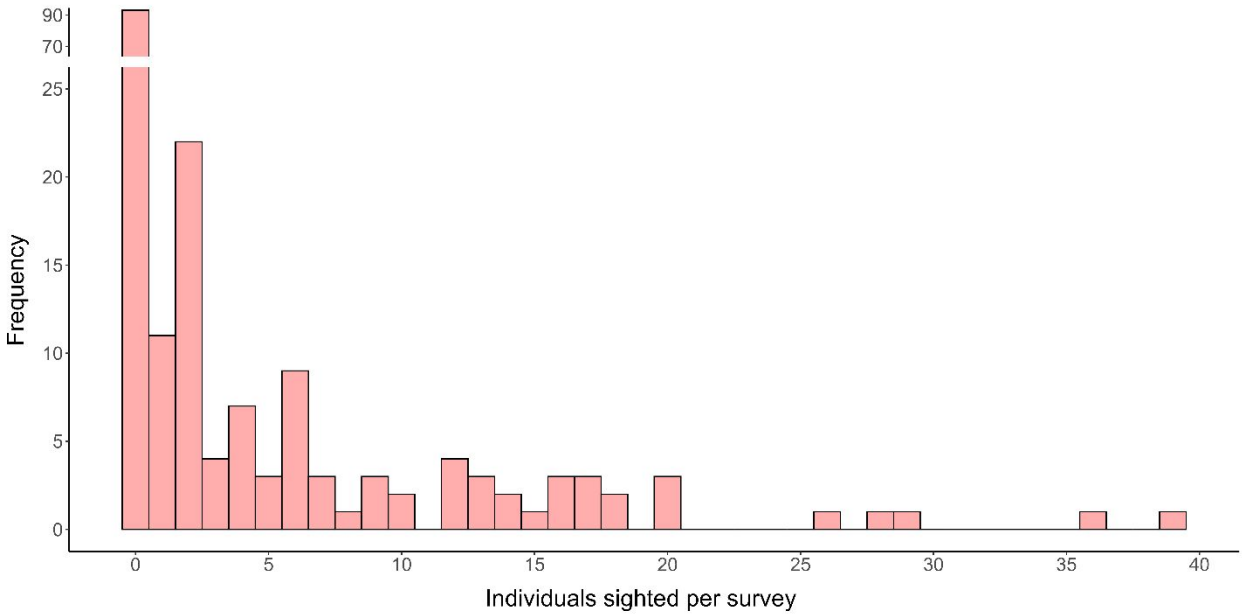

FIGURE 5 Frequency distribution of the count data (number of whales sighted per survey) for the analysis conducted in the 2012-2017 period.

The best-ranked time-series model of 27 alternatives presented a negative binomial likelihood, as did the next five models, and included a long-term trend represented by a second-degree polynomial function of time for Julian days, which is a random seasonal effect of the bimester of the year and an autoregressive effect of Order 4, operating as the interannual component (Table 8).

382 **TABLE 8** Time series model alternatives for fin whale encounter rates (*ER*) in the Eastern Midriff Islands
383 Region, Gulf of California. The models consider the fixed effects of time (as represented in Julian days -
384 *JD*), the random seasonal effects (*s*) of the bimester of the year (*BY*), the autoregressive effects (*ar*) of
385 the Julian bimester (*JB*), and the autoregressive effects on a yearly (*Y*) scale. The indices of the
386 autoregressive effects denote the order of the effect in the corresponding time scale. A mean predictive
387 integral transform (PIT) lower than 0.5 indicates some over estimation. The models are sorted from
388 lowest to highest on the Watanabe-Akaike Information Criterion (WAIC), while the difference between
389 each model's WAIC scores and the best model is shown in the last column.

No.	Formula	PIT	WAIC	ΔWAIC
1	$log(ER) \sim JD + JD^2 + s(BY) + ar_1(JB) + ar_3(Y)$	0.3058	7285.969	0
2	$log(ER) \sim JD + JD^2 + s(BY) + ar_2(JB) + ar_4(Y)$	0.3059	7286.123	0.154
3	$log(ER) \sim JD + JD^2 + s(BY) + ar_2(JB) + ar_2(Y)$	0.3059	7286.129	0.16
4	$log(ER) \sim JD + JD^2 + s(BY) + ar_2(JB) + ar_1(Y)$	0.3057	7286.306	0.337
5	$log(ER) \sim JD + JD^2 + s(BY) + ar_1(JB) + ar_2(Y)$	0.3057	7286.393	0.424
6	$log(ER) \sim JD + JD^2 + s(BY) + ar_1(JB) + ar_4(Y)$	0.3056	7286.482	0.513
7	$log(ER) \sim JD + JD^2 + s(BY) + ar_2(JB) + ar_3(Y)$	0.3058	7286.629	0.66
8	$log(ER) \sim JD + s(BY) + ar_2(JB) + ar_2(Y)$	0.3064	7286.672	0.703
9	$log(ER) \sim JD + s(BY) + ar_2(JB) + ar_3(Y)$	0.3063	7286.69	0.721
10	$log(ER) \sim JD + JD_2 + s(BY) + ar_1(JB) + ar_1(Y)$	0.3057	7286.796	0.827

390

391 The best model explained 45% of the total variance and captured the general patterns observed in the
392 data, including important increases in encounter rates for the cold seasons of 2010, 2013-2014, and
393 2014-2015 (Fig. 6). The long-term predictions showed a peak in 2013 and a steady decrease from 2014 to
394 2017.

395

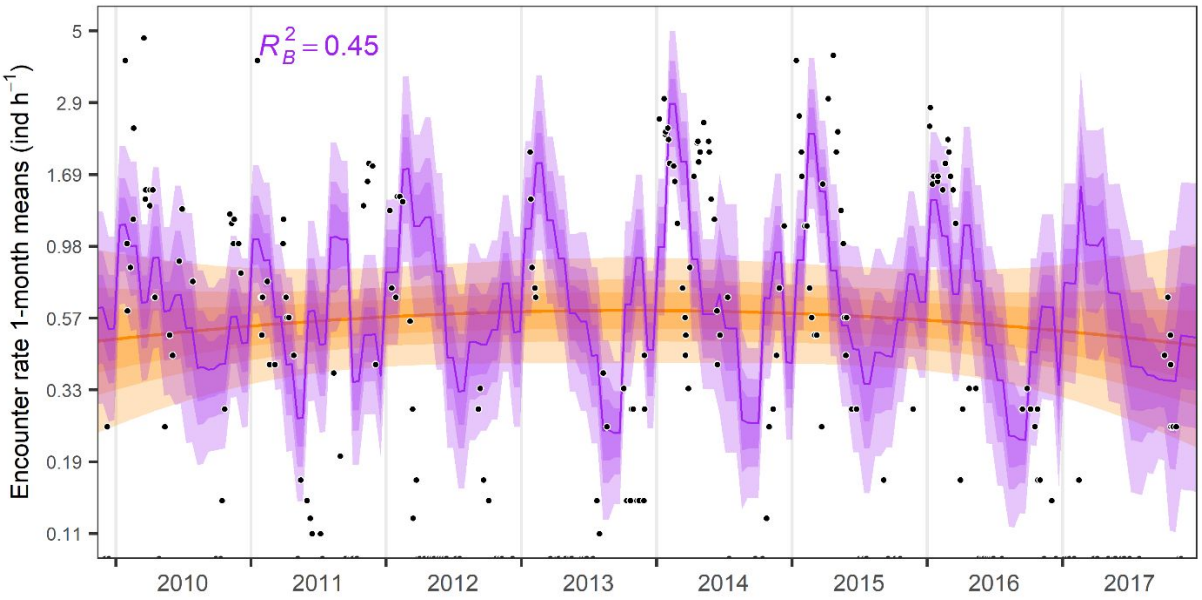

396 **FIGURE 6** Time series for fin whale encounter rates (logarithmic scale, black dots). The purple ribbons
397 (95%-, 75%-, and 50%-CI in incremental darkness) and purple line (median) represent the global
398 predictions of the best model, including all corresponding effects. The orange ribbon (95%-, 75%-, and
399 50%-CI in incremental darkness) and orange line (median) represent the partial long-term trend only.

400

401 On the seasonal scale, the partial predictions showed an increase in encounter rates for November-
402 December, which lasted until March-April and reached a peak in January-February (Fig. 7).

403

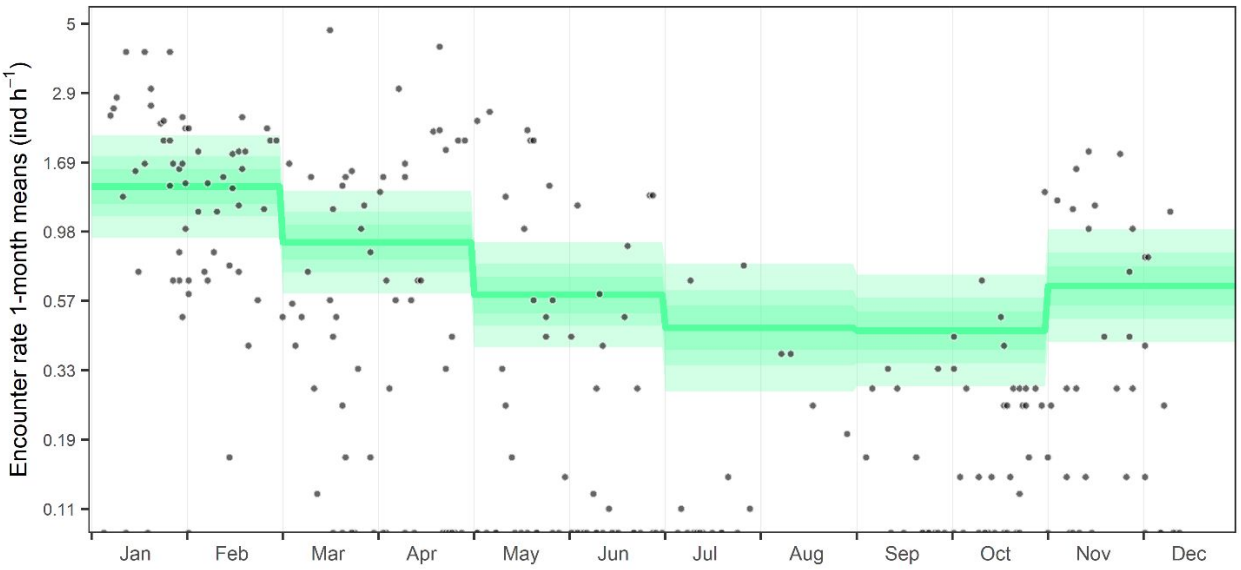

404

405 **FIGURE 7** Partial seasonal effects of the bimester of the year on fin whale encounter rates. The green line
406 corresponds to the median prediction and the green ribbons correspond to the 95%-, 75%-, and 50%-
407 credible intervals, in incremental darkness.

408

409 The interannual autoregressive effects on fin whale encounter rates were positive in 2010 and 2014-
410 2017; whereas the periods 2009 and 2011-2013 presented negative effects (Fig. 8).

411

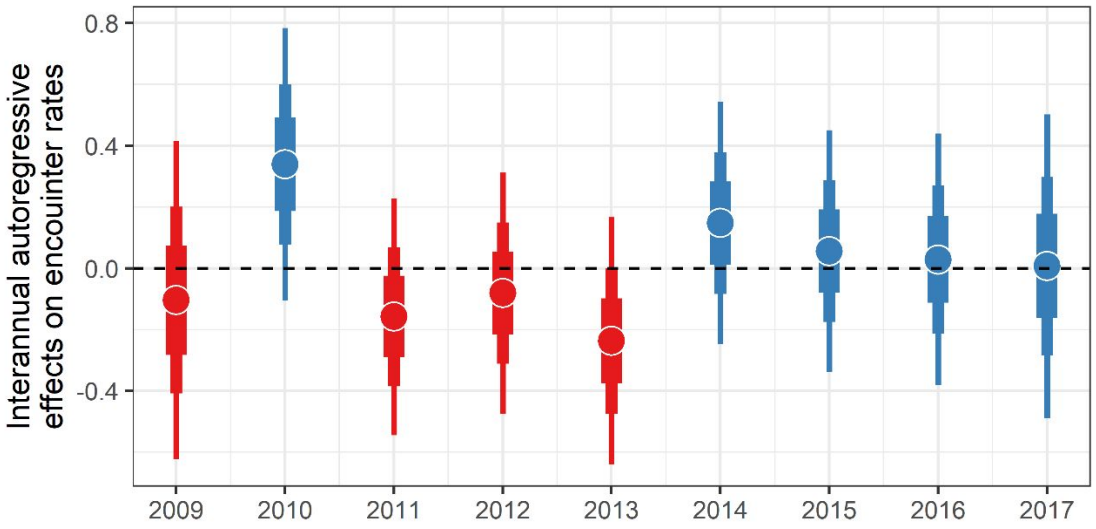

412

413 **FIGURE 8.** Interannual autoregressive effects on fin whale encounter rates (1-month running means),

414 thus representing the interannual variations. Vertical bars show the median value only.

415

416 **4 | DISCUSSION**

417 Our superpopulation abundance estimate ($\hat{N}$ = 462 (SE_{Un} = 41.45, 95%CI [381 – 543]), which is the

418 number of fin whales that visited the study area during the years 2009-2017, is similar to most of the

419 previous abundance estimates. It is lower than the 829 (95% CI [594-3,229]) obtained from distance

420 sampling in the entire Gulf of California (Gerrodette & Palacios, 1996). However, it is comparable to the

421 estimate of 659 (95% CI [458-1043]) based on mark-recapture models from surveys undertaken mostly

422 on the western coast of the gulf and a few surveys in Kino Bay (Díaz-Guzmán, 2006). The value is well

423 within the range of the estimate of 572 (95% CI [106-2,338]) derived from genetic data from tissue

424 samples collected in the northern and southwestern gulf (Montesinos-Laffont, 2016). Also, there is an

425 unpublished POPAN abundance estimate of 325 individuals (95% CI [248-427]) for the Gulf of California

426 using photo-identification data from 2010-2015 from different regions, not just the EMIR (Pardo et al.,

2017). This report also presented abundance estimates with other methods like aerial distance sampling and mark-recapture with genetic data, reporting a historic abundance estimate of 346 individuals (95% CI [170-750]) (Pardo et al., 2017). All these estimates are close to the value presented in this work. We conclude that a large percentage of the resident fin whale population passed through the EMIR during our study period.

Regarding the Jolly-Seber model's assumption of equal probability of capture for both marked and unmarked individuals, we did not find evidence for a lack of fit to the CJS model. However, we experimentally observed that even though there was no statistical evidence in GOF testing of issues with transience nor trap dependence, the inclusion of transience to our model improved the fit and QAICc ranking of those models in comparison to the ones that did not, generating better real and derived estimates.

In terms of the identifiability of the photo-identifications used for the photo-comparison process, we relied not only on dorsal fin shape and nicks but also on scars and skin pigmentation patterns. We do acknowledge that we did not include a separate photo for the chevron and blaze for each individual. In our experience, the dorsal area around the dorsal fin seems to contain enough information for reliable photo-comparisons in this population. Given both the potential for human error during the photo-comparison and potential issues with the quality of the photographs, we only analyzed digital photographs of the highest quality (see *Methods*). We did address the issue of some individuals being more distinctive than others by categorizing and describing the characteristics of each photograph in our catalog following recommendations in the literature (Friday et al., 2000; Urian et al 2014) and removing the individuals with photo-identifications having low quality and distinctiveness (Q3 and D3 respectively) from mark-recapture analysis. We note, however, that photo-identifications with Q3 quality still satisfied our minimum requirements for inclusion in the photo-compasion process.

450 We additionally calculated a mark ratio to address the issue of identifiability, looking to reduce potential
451 sources of bias on our estimates, by removing about half of the individuals in our catalog, those with the
452 lowest quality photographs and distinctiveness. We later used the mark ratio to inflate our estimates as
453 is recommended in the literature (Urian et al., 2015), recognizing the problem of how some whales are
454 easier to match than others. With regard to the duration of the capture events when compared to the
455 time interval that elapsed between them, in the present study each sampling occasion (ten to eleven
456 months) was longer than the interval between them (one month). Thus, violation of this assumption
457 could have biased our estimates. However, as reported in a simulation study (O'Brien et al., 2005),
458 violation of this assumption increases precision and does not significantly increase bias in parameter
459 estimates, as long as the recapture probability is higher than 0.2, which was the case for the present
460 study. The aforementioned authors recommended using sampling periods that maximize sample size
461 and increase recapture rate, which we did here. Additionally, regarding the assumption of individuals
462 being a random sample of the population visiting the region, goodness-of-fit testing showed no evidence
463 of transience. However, including transience into our models yielded better explanatory power to our
464 models. This meant that even though GOF testing did not statistically detect evidence of transience in
465 our data, it was still present. This difference in behavior can bias survival and abundance estimates so it
466 was addressed in our modelling to reduce its impact. During the surveys, there was no indication to
467 photograph some whales more than others. The objective was to photograph as many different
468 individuals in each sighting as was practically possible.

469 Previous mark-recapture studies conducted on this population in the Gulf of California did not report
470 survival estimates. Given that the abundance obtained by the use of the POPAN model depends on both
471 how many animals enter the population over time and how many of them survive, a bias in ϕ would
472 impact estimates of *N* (Schwarz & Arnason, 1996; Williams et al., 2002). The survival estimates obtained
473 from the CJS model, which explicitly model transience, were comparable to the ones obtained from our

474 POPAN model. The "multiple recaptures" class in the CJS model had a $\phi = 0.915$ (SE = 0.034, 95% CI
475 [0.819– 0.962]). In comparison to other studies, the survival estimates obtained here are lower than
476 what has been estimated for fin whales in the Gulf of St Lawrance in Canada with means of 0.946 (95%
477 CI [0.91-0.967]) (Schleimer et al., 2019) and 0.955 (95% CI [0.936 – 0.969]) (Ramp et al., 2014). The value
478 is closer to what has been estimated for the norhwestern Mediterranean, a value of 0.916 (95% CI [0.773
479 – 0.972]) (Zanardelli et al., 2022), with the difference that our confidence limits are narrower. It is worth
480 noting that this value is relatively low for what is expected for such a long-lived species.

481 Given the foregoing, it could be concluded that our study area represents an important corridor for the
482 fin whales, and some of them show preference to stay in the area longer and visit it more often. Some
483 studies contribute to this fact, indicating that the Midriff Islands Region is an important corridor for the
484 species. It should be noted that eight fin whales that were satellite-tagged in the southwestern Gulf of
485 California have visited the EMIR when moving farther north (Jiménez-López et al., 2019). However, it is
486 unknown both whether there is a substructure in the population and whether part of it only inhabits the
487 southwestern gulf.

488 The annual abundance estimates for the years 2010-2016 showed overlap in their confidence limits
489 suggesting stability in the area. It is worth noting that true abundance may be varying substantially by
490 either inter-annual variability or a positive-negative trend, or a combination of both factors. The INLA
491 analysis did show a slight decrease in the long-term temporal trend. However, these results indicate that
492 this area has served as an important aggregation site for fin whales every year of this study.

493 A 2000-2021 time series analysis revealed that the sea surface chlorophyll-*a* anomaly in the Gulf of
494 California was mostly negative from 2013 to 2019, aside from in the Midriff Islands Region in January-
495 March 2014, October 2014, and March 2015 (García-Fernández et al., 2023). In data obtained from 2002
496 to 2019, the EMIR showed a higher chlorophyll-*a* concentration than other regions (the north, center,

497 south) of the eastern Gulf of California but then presented a decreased concentration in 2013 (Robles-
498 Tamayo et al., 2020). García-Fernández et al. (2023) also reported that Euphausiids, the main prey for fin
499 whales in the gulf, presented a low relative abundance in 2013, which increased progressively until 2019.
500 The 2013-2014 period presented the most sightings and photo-identifications and was also the year
501 during which the most recaptures were recorded by the present study. However, as indicated by the
502 capture-recapture estimates, the abundance obtained showed a constant trend, suggesting that the area
503 continues to be used as an aggregation site in years with chl-*a* changes. The Midriff Islands Region has
504 been described as a refuge for marine megafauna during El Niño years (Ladrón-De-Guevara et al., 2015;
505 Tershy et al., 1991), when most of the Gulf of California retains positive sea surface temperature
506 anomalies (Escalante et al., 2013; Lavín et al., 2003) and low primary productivity (Escalante et al., 2013;
507 García-Fernández et al., 2023; Hakspiel-Segura et al., 2022).

508 The seasonal variation model applied by the present study showed that fin whales were more
509 abundant during the cold season, particularly from January to March, while the lowest encounter rates
510 were found to occur in June (cold-warm season transition) and July (warm season). This coincides with
511 the results of a telemetry study, which reported that two out of eight satellite-tagged fin whales visited
512 the EMIR during the cold season. Interestingly, most of the observations were related to foraging
513 behavior (Jiménez-López et al., 2019), which coincides with the surface lunge feeding behavior observed
514 in 9.7% of the fin whale sightings registered by the present study. Moreover, peak fin whale encounter
515 rates in the Ballenas Channel, in the western Midriff Islands Region, occur during the warm season
516 (Ladrón-De-Guevara et al., 2015), which coincides with the decrease in the occurrence of fin whales
517 observed in our study area and may suggest a seasonal movement from east to west within the Midriff
518 Islands Region.

519 The higher abundance of fin whales observed during the cold season than the warm season in the EMIR
520 probably corresponds to the highly seasonal upwelling regime of the Gulf of California's eastern coast

(Escalante et al., 2013; Hakspiel-Segura et al., 2022; Lluch-Cota, 2000; Robles-Tamayo et al., 2020; Santamaría-del-Ángel et al., 1994). During the cold season, strong northwesterly winds cause upwelling on the eastern coast (Lluch-Cota, 2000) and, as a consequence, the sea surface temperature is lower and phytoplankton production is higher than during the warm season (Álvarez-Molina et al., 2013).

The superpopulation estimate and the temporal trends in encounter rates for fin whales in the EMIR confirm that it is an important seasonal aggregation site and a hotspot for the species, on an interannual scale, in the Gulf of California, as has been stated for the Midriff Islands Region by previous studies (Díaz-Guzmán, 2006; Enríquez-Paredes, 1996; Ladrón-De-Guevara et al., 2015; Tershy et al., 1990; Pardo et al., 2017). Protected by Mexican law (SEMARNAT, 2019), fin whales are a conservation priority. Our results provide additional information on the ecology of this important species in the EMIR, thus we recommend it should be considered in future conservation plans for fin whales in the Gulf of California.

ACKNOWLEDGMENTS

This project was conducted as part of the Marine Mammal Program at Prescott College Kino Bay Center for Cultural and Ecological Studies, A.C. We thank Lorayne Meltzer (Director of the Kino Bay Center) for her support for all the activities conducted by the Marine Mammal Program. Data collection was carried out under the scientific permit SGPA/DGVS/000612/18 issued by the *Secretaría de Medio Ambiente y Recursos Naturales* (Environment and Natural Resources Ministry). We thank Dr. Jorge Urbán-Ramírez (Marine Mammal Research Program at the Autonomous University of Baja California Sur, PRIMMA-UABCS) for allowing us to carry out our activities under his scientific permit. HPP owes special thanks to Cosme Damián Becerra for his invaluable support as boat captain and collaborator for all the years in which we have conducted surveys. We thank Anna Schleimer for her advice on result interpretation using specific code for POPAN abundance analysis. We are very grateful to The David and Lucile Packard

Foundation and Prescott College for their funding support throughout the duration of this study. JAS received an M.Sc., with a full scholarship from CONACYT (No. 769396), while MAP was funded by CICESE (Internal Project No. 691–113) during the preparation of this manuscript. Benjamin Stewart proofread the manuscript. Finally, we thank Dr. Philip Hammond and two anonymous reviewers for their revisions, which helped to improve the manuscript substantially.

AUTHOR CONTRIBUTIONS

Joel A. Arredondo-Sáinz: Investigation; formal analysis; visualization; writing—original draft. **Héctor Pérez-Puig:** Conceptualization; data curation; funding acquisition; investigation; methodology; formal analysis, project administration; resources; supervision; writing—review and editing. **Mario A. Pardo:** Formal analysis, methodology, software, supervision, writing—review and editing. **Gisela Heckel:** Conceptualization; methodology; project administration; supervision; writing—original draft; writing—review and editing.

ORCID

Joel A. Arredondo-Sáinz https://orcid.org/0000-0002-0081-2426

Héctor Pérez-Puig https://orcid.org/0000-0002-8858-2716

Mario A. Pardo https://orcid.org/0000-0003-1248-3399

Gisela Heckel https://orcid.org/0000-0002-6003-7898

REFERENCES

Agler, B.A., Beard, J.A., Bowman, R.S., Corbett, H.D., Frohock, S.E., Hawvermale, M.P., Katona, S.K., Sadove, S.S., & Seipt, I.E. (1990). Fin whale (*Balaenoptera physalus*) photographic identification: methodology and preliminary results from the western north Atlantic. *Reports of the International Whaling Commission (Special Issue 12)*, 349-356.

Akaike, H. (1985). Prediction and entropy. In A.C. Atkinson & S.E. Fienberg (Eds.), A celebration of statistics: the ISI centenary volume (pp. 1-24). Springer. https://doi.org/10.1007/978-1-4613-8560-8_1

Allen, K.R. (1977). Updated estimates of fin whale stocks. *Reports of the International Whaling Commission*, 27, 221.

Álvarez-Borrego, S., & Lara-Lara, J.R. (1991). The physical environment and primary productivity of the Gulf of California. In J.P. Dauphin & B. Simoneit (Eds.), The gulf and peninsular province of the Californias (pp. 555-567). American Association of Petroleum Geologists. https://doi.org/10.1306/M47542C26

Álvarez-Borrego, S. (2010). Physical, chemical, and biological oceanography of the Gulf of California. In R.C. Brusca (Eds.), The Gulf of California: biodiversity and conservation (pp. 24-48). The University of Arizona Press.

584 Álvarez-Molina, L.L., Álvarez-Borrego, S., Lara-Lara, J.R., & Marinone, S.G. (2013). Annual and semiannual
585 variations of phytoplankton biomass and production in the central Gulf of California estimated from
586 satellite data. *Ciencias Marinas*, 39(2), 217-230. https://doi.org/10.7773/cm.v39i2.2189
587
588 Amstrup, C.S., McDonald, T.L., & Manly, B.F.J. (2005). *Handbook of capture-recapture analysis*. Princeton
589 University Press.
590
591 Anderson, D.W., Godínez-Reyes, C.R., Velarde, E., Ávalos-Téllez, R., Ramírez-Delgado, D., Moreno-Prado,
592 H., Bowen, T., Gress, F., Trejo-Ventura, J., Adrean, L., & Meltzer, L. (2017). Brown pelicans, *Pelecanus*
593 *occidentalis californicus* (Aves: Pelecanidae): Five decades with ENSO, dynamic nesting, and
594 contemporary breeding status in the gulf of California. *Ciencias Marinas*, 43(1), 1-34.
595 https://doi.org/10.7773/cm.v43i1.2710
596
597 Bérubé, M., Urbán-Ramírez, J., Dizon, A.E., Brownell Jr., R.L., & Palsbøll, P.J. (2002). Genetic identification
598 of a small and highly isolated population of fin whales (*Balaenoptera physalus*) in the Sea of Cortez,
599 México. *Conservation Genetics*, 3, 183-190. https://doi.org/10.1023/A:1015224730394
600
601 Burgos-Othón, T.A. (2018). Biomasa y producción fitoplanctónicas derivadas de satélite en la parte
602 central del Golfo de California, en 2002-2017 (Phytoplankton biomass and production derived from
603 satellite in the central Gulf of California, from 2002-2017) [Unpublished master's thesis]. Centro de
604 Investigación Científica y de Educación Superior de Ensenada, Baja California.
605
606 Burnham, K., & Anderson, D.R. (2002). *Model selection and multi-model inference, 2nd edn*. Springer.

607

608 Cooke, J.G. (2018). *Balaenoptera physalus*. The IUCN Red List of Threatened Species 2018:
609 e.T2478A50349982. https://dx.doi.org/10.2305/IUCN.UK.2018-2.RLTS.T2478A50349982.en

610

611 Darling, J.D., & Morowitz, H. (1986). Census of "Hawaiian" humpback whales (*Megaptera novaeangliae*)
612 by individual identification. *Canadian Journal of Zoology*, 64(1), 105-111. https://doi.org/10.1139/z86-
613 017

614

615 Díaz-Guzmán, C.F. (2006). Abundancia y movimientos del rorcual común, *Balaenoptera physalus*, en el
616 Golfo de California (Abundance and movements of the fin whale, *Balaenoptera physalus,* in the Gulf of
617 California) [Unpublished master's thesis]. Universidad Nacional Autónoma de México.

618

619 Enríquez-Paredes, L.M. (1996). Ocurrencia, movimientos, estructura social y tamaño de las agregaciones
620 de rorcual común (*Balaenoptera physalus*) en el Golfo de California, México (Occurrence, movements,
621 social structure and size of aggregations of the fin whale (*Balaenoptera physalus*) in the Gulf of
622 California, Mexico) [Unpublished bachelor's thesis]. Universidad Autónoma de Baja California Sur.

623

624 Escalante, F., Valdez-Holguín, J.E., Álvarez-Borrego, S., & Lara-Lara, J.R. (2013). Temporal and spatial
625 variation of sea surface temperature, chlorophyll *a*, and primary productivity in the Gulf of California.
626 *Ciencias Marinas*, 39(2), 203-215. https://doi.org/10.7773/cm.v39i2.2233

627

628 Espinosa-Carreón, T.L., & Valdez-Holguín, J.E. (2007). Variabilidad interanual de clorofila en el Golfo de
629 California (Interannual chlorophyll variability in the Gulf of California). *Ecología Aplicada* 6(1,2), 83-92.
630 https://doi.org/10.21704/rea.v6i1-2.344
631
632 Friday, N., Smith, T.D., Stevick ,P.T., Allen, J. (2000) Measurement of photographic quality and individual
633 distinctiveness for the photographic identification of humpback whales, *Megaptera novaeangliae*.
634 Marine Mammal Science, 16(2), 355-374. https://doi.org/10.1111/j.1748-7692.2000.tb00930.x
635
636 García-Fernández, F., Gómez-Gutiérrez, J., De-Silva-Dávila, R., Hakspiel-Segura, C., Ambriz-Arreola, I.,
637 Martínez-López, A., Sánchez-Uvera, A.R., Hernández-Rivas, M.E., & Robinson, C.J. (2023). Interannual
638 response of euphausiid community abundance during the anomalous warming period (2014-2016) in the
639 Gulf of California. *Progress in Oceanography*, 212, 102994.
640 https://doi.org/10.1016/j.pocean.2023.102994
641
642 Gerrodette, T., & Palacios, D. (1996). *Estimates of cetacean abundance in EEZ waters of the eastern*
643 *tropical Pacific* (NOAA Administrative Report LJ-96-10). U.S. Department of Commerce.
644
645 Gimenez, O., Lebreton, J.-D., Choquet, R., & Pradel, R. (2018). R2ucare: An r package to perform
646 goodness-of-fit tests for capture–recapture models. *Methods in Ecology and Evolution*, 9(7), 1749-1754.
647 https://doi.org/10.1111/2041-210X.13014
648
649 Gómez-Rubio, V. (2020). *Bayesian inference with INLA, 1st ed.* Taylor & Francis, CRC Prees
650

651 Hakspiel-Segura, C., Martínez-López, A., Delgado-Contreras, J.A., Robinson, C.J., & Gómez-Gutiérrez, J.
652 (2022). Temporal variability of satellite chlorophyll-*a* as an ecological resilience indicator in the central
653 region of the Gulf of California. *Progress in Oceanography*, 205, 102825.
654 https://doi.org/10.1016/j.pocean.2022.102825
655

656 Hidalgo-González, R.M., & Álvarez-Borrego, S. (2001). Chlorophyll profiles and the water column
657 structure in the Gulf of California. *Oceanologica Acta*, 24(1), 19-28. https://doi.org/10.1016/S0399-
658 1784(00)01126-9
659

660 Jefferson, T.A., Webber, M.A., Pitman, R.L., & Gorter, U. (2015). *Marine mammals of the world. A*
661 *comprehensive guide to their identification*. Elsevier.
662

663 Jiménez-López, M.E., Palacios, D.M., Jaramillo-Legorreta, A., Urbán-Ramírez, J., & Mate, B.R. (2019). Fin
664 whale movements in the Gulf of California, Mexico, from satellite telemetry. *PLoS ONE*, 14, e0209324.
665 https://doi.org/10.1371/journal.pone.0209324
666

667 Jolly, G.M. (1965). Explicit estimates from capture-recapture data with both death and immigration - a
668 stochastic model. *Biometrika*, 52(1-2), 225-248. https://doi.org/10.1093/biomet/52.1-2.225
669

670 Laake, J.L. (2013). *RMark: An R Interface for Analysis of Capture-Recapture Data with MARK. AFSC*
671 *Processed Rep. 2013-01.* Alaska Fisheries Science Center, NOAA, National Marine Fisheries Service.
672 https://apps-afsc.fisheries.noaa.gov/Publications/ProcRpt/PR2013-01.pdf

673

674 Ladrón-De-Guevara, P., Heckel, G., & Lavaniegos, B.E. (2015). Spatial and temporal occurrence of fin
675 whales (*Balaenoptera physalus*) and euphausiids (*Nyctiphanes simplex*) in the Ballenas channel, Gulf of
676 California, Mexico. *Ciencias Marinas*, 41(2), 125-142. https://doi.org/10.7773/cm.v41i2.2497

677

678 Lavín, M.F., Palacios-Hernández, E., & Cabrera, C. (2003). Sea surface temperature anomalies in the Gulf
679 of California. *Geofisica Internacional*, 42, 363-375.
680 https://doi.org/10.22201/igeof.00167169p.2003.42.3.956

681

682 Lebreton, J.D., Burnham, K.P., Clobert, J., & Anderson, D.R. (1992). Modeling survival and testing
683 biological hypotheses using marked animals—a unified approach with case studies. *Ecological*
684 *Monographs*, 62(1), 67-118. https://doi.org/10.2307/2937171

685

686 Lluch-Cota, S.E. (2000). Coastal upwelling in the eastern Gulf of California. *Oceanologica Acta*, 23(6), 731-
687 740. https://doi.org/10.1016/S0399-1784(00)00121-3

688

689 Lluch-Cota, S.E., Aragón-Noriega, E.A., Arreguín-Sánchez, F., Aurioles-Gamboa, D., Bautista-Romero, J.J.,
690 Brusca, R.C., Cervantes-Duarte, R., Cortés-Altamirano, R., Del-Monte-Luna, P., Esquivel-Herrera, A.,
691 Fernández, G., Hendrickx, M.E., Hernández-Vázquez, S., Herrera-Cervantes, H., Kahru, M., Lavín, M.,
692 Lluch-Belda, D., Lluch-Cota, D.B., López-Martínez, J., Marinone, S.G., Nevárez-Martínez, M.O., Ortega-
693 García, S., Palacios-Castro, E., Parés-Sierra, A., Ponce-Díaz, G., Ramírez-Rodríguez, M., Salinas-Zavala,
694 C.A., Schwartzlose, R.A., & Sierra-Beltrán, A.P. (2007). The Gulf of California: Review of ecosystem status

and sustainability challenges. *Progress in Oceanography*, 73(1), 1-26. https://doi.org/10.1016/j.pocean.2007.01.013

Martínez-Villalba, M.G. (2008). Distribución y abundancia de la ballena de aleta (*Balaenoptera physalus*) en aguas adyacentes a Guaymas y algunas inferencias ecológicas generales sobre esta especie en el Golfo de California (Distribution and abundance of fin whales (*Balaenoptera physalus*) in waters surrounding Guaymas, and some general ecological inferences about the species in the Gulf of California) [Unpublished master's thesis]. Universidad Nacional Autónoma de México.

Montesinos-Laffont, A.I. (2016). Evidencia genética de estabilidad en la abundancia de la población del rorcual común del Golfo de California, México (Genetic evidence of stability in the abundance of the Gulf of California fin whale population) [Unpublished master's thesis]. Universidad Autónoma de Baja California.

O'Brien, S., Robert, B., & Tiandry, H. (2005). Consequences of violating the recapture duration assumption of mark – recapture models : a test using simulated and empirical data from an endangered tortoise population. *Journal of Applied Ecology*, 42(6), 1096-1104. https://doi.org/10.1111/j.1365-2664.2005.01084.x

Ohsumi, S., & Wada, S. (1974). Status of whale stocks in the North Pacific, 1972. *Reports of the International Whaling Commission (Special Issue 6)*, 24, 114-126.

Pardo, M., Gendron, D., Carone, E., Jiménez, E., Busquets-Vass, G., Urbán, J., Viloria, L., Enríquez, L., Mata, R. (2017). Determinación del estado y dinámica poblacional del rorcual común en el Golfo de

718 California. Informe final. Programa de Conservacion de Especies en Riesgo (PROCER). La Paz, Baja
719 California Sur, México [Status and population dynamics of fin whales in the Gulf of California. Final
720 report. Program for the Conservation of Species at Risk].
721
722 Pérez-Álvarez, M., Kraft, S., Segovia, N.I., Olavarría, C., Nigenda-Morales, S., Urbán-Ramírez, J., Viloria-
723 Gómora, L., Archer, F.I., Moraga, R., Sepúlveda, M., Santos-Carvallo, M., Pavez, G., & Poulian, E. (2021).
724 Contrasting phylogeographic patterns among northern and southern hemisphere fin whale populations
725 with new data from the Southern Pacific. *Frontiers in Marine Science*, 8, 630233.
726 https://doi.org/10.3389/fmars.2021.630233
727
728 R Core Team. 2023. R: A language and environment for statistical computing. R Foundation for Statistical
729 Computing. Vienna, Austria. http://www.R-project.org/.
730
731 Ramp, C., Delarue, J., Bérubé, M., Hammond, P.S., & Sears, R. (2014). Fin whale survival and abundance
732 in the Gulf of St. Lawrence, Canada. *Endangered Species Research*, 23(2), 125-132.
733 https://doi.org/10.3354/esr00571
734
735 Ravishanker, N., Raman, B., & Soyer, R. (2023). *Dynamic time series models using R-INLA: An applied*
736 *perspective, 1st ed.* CRC Press, Taylor & Francis, Chapman & Hall.
737
738 Rivera-León, V.E., Urbán-Ramírez, J., Mizroch, S.A., Brownell Jr., R.L., Oosting, T., Hao, W., Palsboll, P.J., &
739 Bérubé, M. (2019). Long-term isolation at a low effective population size greatly reduced genetic

diversity in Gulf of California fin whales. *Scientific Reports*, 9, 12391. https://doi.org/10.1038/s41598-019-48700-5

Robles-Tamayo, C.M., García-Morales, R., Valdez-Holguín, J.E., Figueroa-Preciado, G., Herrera-Cervantes, H., López-Martínez, J., & Enríquez-Ocaña, L.F. (2020). Chlorophyll *a* concentration distribution on the mainland coast of the Gulf of California, Mexico. *Remote Sensing*, 12, 1335. https://doi.org/10.3390/rs12081335

Rue, H., Martino, S., & Chopin, N. (2009). Approximate Bayesian inference for latent Gaussian models by using integrated nested Laplace approximations. *Journal of the Royal Statistical Society, Series B*, 71(2), 319-392. https://doi.org/10.1111/j.1467-9868.2008.00700.x

Santamaría-del-Ángel, E., Álvarez-Borrego, S., & Müller-Karger, F.E. (1994). Gulf of California biogeographic regions based on coastal zone color scanner imagery. *Journal of Geophysical Research*, 99(C4), 7411-7421. https://doi.org/10.1029/93JC02154

Sarasota Dolphin Research Program. (2005) Field Techniques and Photo-Identification Handbook. Chicago Zoological Socierty and Dolphin Biology Rearch Institute c/o Mote Marine Laboratory. Sarasota, Florida, USA.

Schleimer, A., Ramp, C., Delarue, J., Carpentier, A., Bérubé, M., Palsboll, P.J., Sears, R., & Hammond, P.S. (2019). Decline in abundance and apparent survival rates of fin whales (*Balaenoptera physalus*) in the northern Gulf of St. Lawrence. *Ecology and Evolution*, 9, 4231-4244. https://doi.org/10.1002/ece3.5055

Schwarz, C.J., & Arnason, A.N. (1996). A general methodology for the analysis of capture-recapture experiments in open populations. *Biometrics*, 52, 860-873. https://doi.org/10.2307/2533048

Seber, G.A.F. (1965). A note on the multiple-recapture census. *Biometrika*, 52(1-2), 249-259. https://doi.org/10.2307/2333827

SEMARNAT. (2019). Modificación del Anexo Normativo III, Lista de especies en riesgo de la Norma Oficial Mexicana NOM-059-SEMARNAT-2010, Protección ambiental-Especies nativas de México de flora y fauna silvestres-Categorías de riesgo y especificaciones para su inclusión, exclusión o cambio-Lista de especies en riesgo, publicada el 30 de diciembre de 2010 *Diario Oficial de la Federación, 14 Noviembre 2019.*

Tershy, B.R., Breese, D., & Strong, C. (1990). Abundance, seasonal distribution and population composition of Balaenopterid whales in the Canal de Ballenas, Gulf of California, México. *Reports of the International Whaling Commission*, (Special Issue 12), 369-375.

Tershy, B.R., Breese, D., & Alvarez-Borrego, S. (1991). Increase in cetacean and seabird numbers in the Canal de Ballenas during an El Niño-Southern Oscillation event. *Marine Ecology Progress Series*, 69, 299-302.

783 Tershy, B.R., Urbán-Ramírez, J., Breese, D., Rojas-Bracho, L., & Findley, L.T. (1993). Are fin whales
784 resident to the Gulf of California? *Revista de Investigación Científica de la Universidad Autónoma de Baja*
785 *California Sur. Serie Ciencias del Mar*, 1, 69-72.
786
787 Urbán-Ramírez, J., Rojas-Bracho, L., Guerrero-Ruiz, M., Jaramillo-Legorreta, A., & Findley, L.T. (2005).
788 Cetacean diversity and conservation in the Gulf of California. In J.E. Cartron, G. Ceballos & R.S. Felger
789 (Eds.), Biodiversity, ecosystems, and conservation in northern Mexico (pp. 276-297). Oxford University
790 Press.
791
792 Urian, K., Gorgone, A., Read, A., Balmer, B., Wells, R.S., Berggren, P., Durban, J., Eguchi, T., Rayment, W.,
793 Hammond, P.S. (2015). Recommendations for photo-identification methods used in capture-recapture
794 models with cetaceans. *Marine Mammal Science* , 31(1), 298-321. https://doi.org/10.1111/mms.12141
795
796 White, G.C., & Burnham, K.P. (1999). Program MARK: Survival estimation from populations of marked
797 animals.*Bird Study,*46(Supplement), S120-S139 https://doi.org/10.1080/00063659909477239
798
799 Wickham, H., Averick, M., Bryan, J., Chang, W., McGowan, L.D.A., Francois, R., Grolemund, G., Hayes, A.,
800 Henry, L., Hester, J., Kuhn, M., Pedersen, T.L., Miller, E., Bache, S.M., Müller, K., Ooms, J., Robinson, D.,
801 Seidel, D.P., Spinu, V., Takahashi, K., Vaughan, D., Wilke, C., Woo, K., & Yutani, H. (2019). Welcome to the
802 tidyverse. *Journal of Open Source Software*, 4(43), 1686. https://doi.org/10.21105/joss.01686
803
804 Wickham, H., Navarro, D., & Pedersen, T.L. (2022). *ggplot2: elegant graphics for data analysis*. Springer.
805

Williams, B.K., Nichols, J.D., & Conroy, M.J. (2002). *Analysis and Management of Animal Populations: Modeling, Estimation and Decision Making*. Academic Press.

Zanardelli, M., Airoldi, S., Bérubé, M., Borsani, J.F., Di-Meglio, N., Gannier, A., Hammond, P.S., Jahoda, M., Lauriano, G., Notarbartolo di Sciara, G., & Panigada, S. (2022). Long-term photo-identification study of fin whales in the Pelagos Sanctuary (NW Mediterranean) as a baseline for targeted conservation and mitigation measures. *Aquatic Conservation: Marine and Freshwater Ecosystems*, 32(9), 1457-1470. https://doi.org/10.1002/aqc.3865

DATA AVAILABILITY

The datasets generated and/or analyzed during the present study are available from the corresponding author on reasonable request.

CODE AVAILABILITY

The code used to analyze the capture histories using the POPAN model both with transience and for the time series data analysis, is available from the corresponding author on reasonable request.

SUPPORTING INFORMATION

Additional supporting information can be found online in the Supporting Information section at the end of this article.

CONFLICT OF INTEREST

828 The authors declare no conflict of interest.

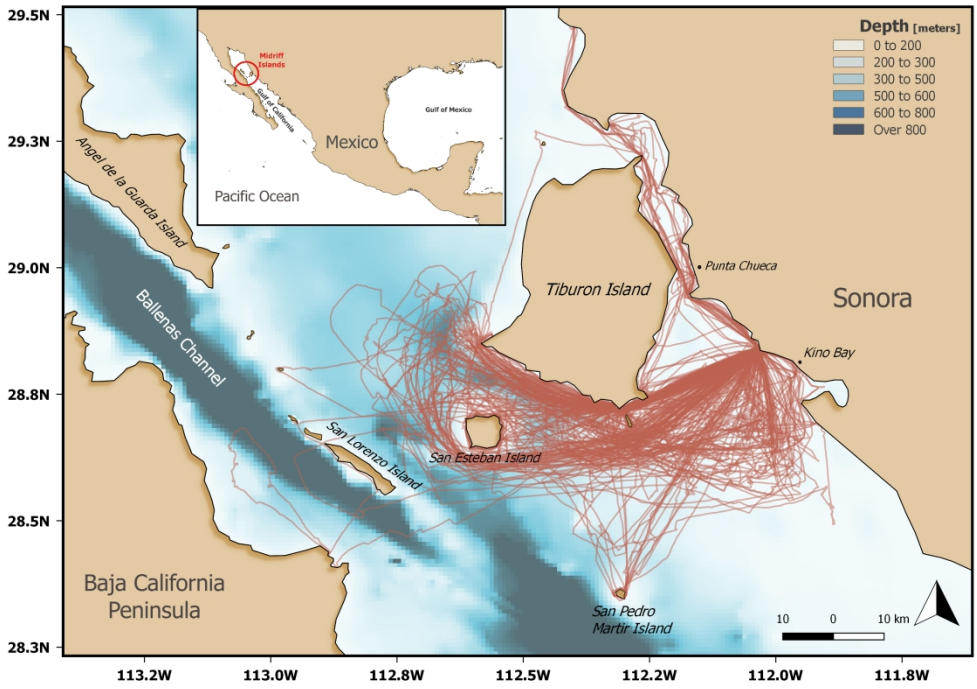

FIGURE 1 Study area in the Eastern Midriff Islands Region in the Gulf of California, Mexico. The GPS tracks in red represent the surveys undertaken from 2012 to 2017.

927x656mm (96 x 96 DPI)

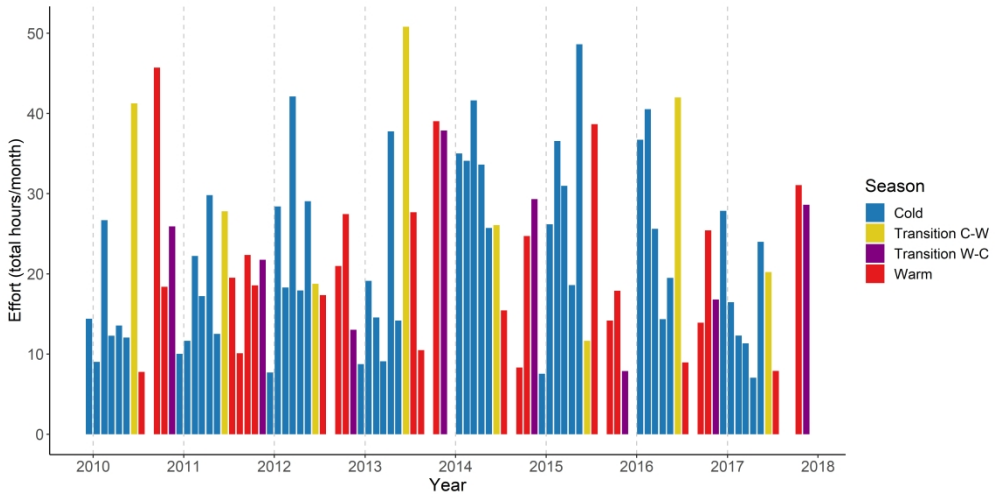

FIGURE 2 Search effort hours per month during the eight years comprising the present study (2009-2017). The data are colored depending on the seasons surveyed. Transition C-W = Transition from cold to warm season; Transition W-C = Transition from warm to cold season.

299x149mm (600 x 600 DPI)

FIGURE 3 Photo-identification recaptures for individual 121 - both left and right side of the dorsal fin. In this particular case, the scar midway up the dorsum helped to confirm the photo-identification recaptures of this individual.

158x158mm (96 x 96 DPI)

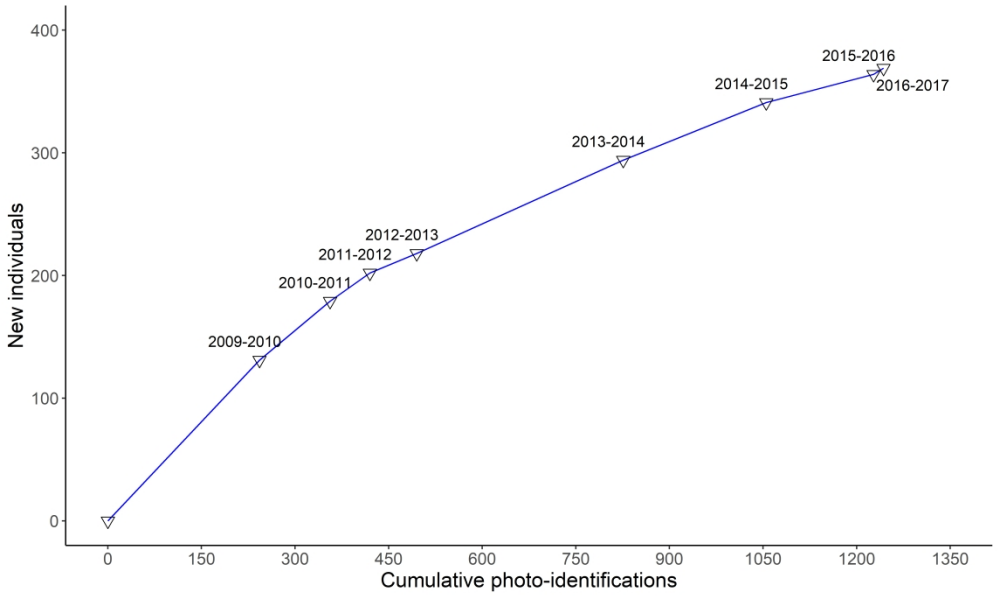

FIGURE 4 Discovery curve for cumulative photo-identified individuals, along with the rate of appearance for new individuals.

254x152mm (600 x 600 DPI)

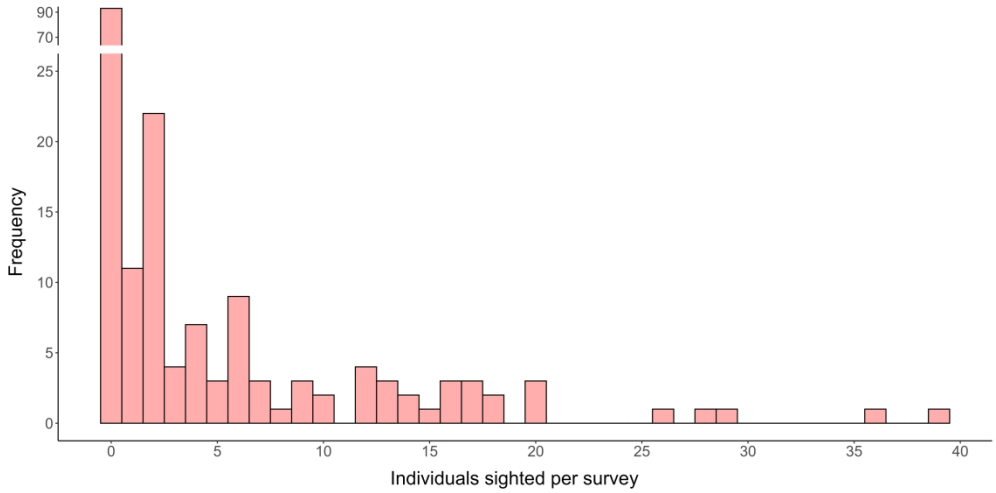

FIGURE 5 Frequency distribution of the count data (number of whales sighted per survey) for the analysis conducted in the 2012-2017 period.

355x177mm (300 x 300 DPI)

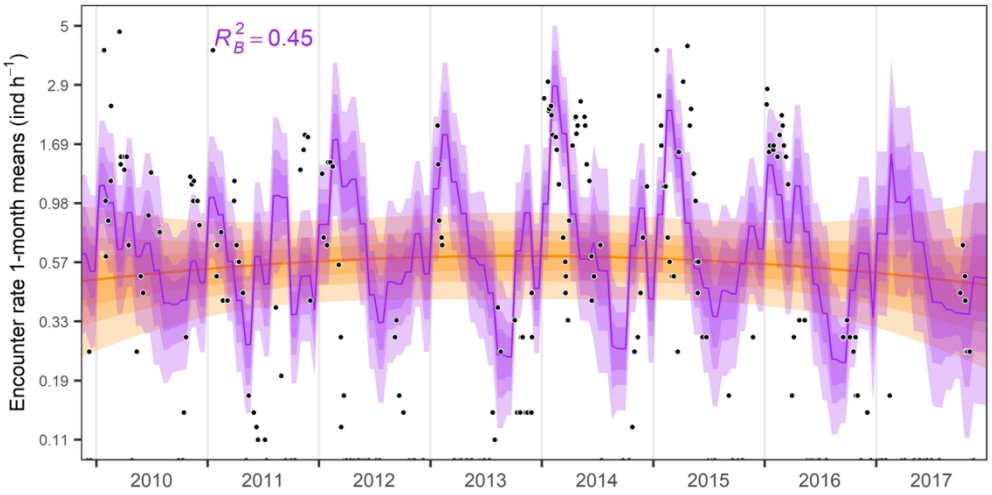

FIGURE 6 Time series for fin whale encounter rates (logarithmic scale, black dots). The purple ribbons (95%-, 75%-, and 50%-CI in incremental darkness) and purple line (median) represent the global predictions of the best model, including all corresponding effects. The orange ribbon (95%-, 75%-, and 50%-CI in incremental darkness) and orange line (median) represent the partial long-term trend only.

139x70mm (300 x 300 DPI)

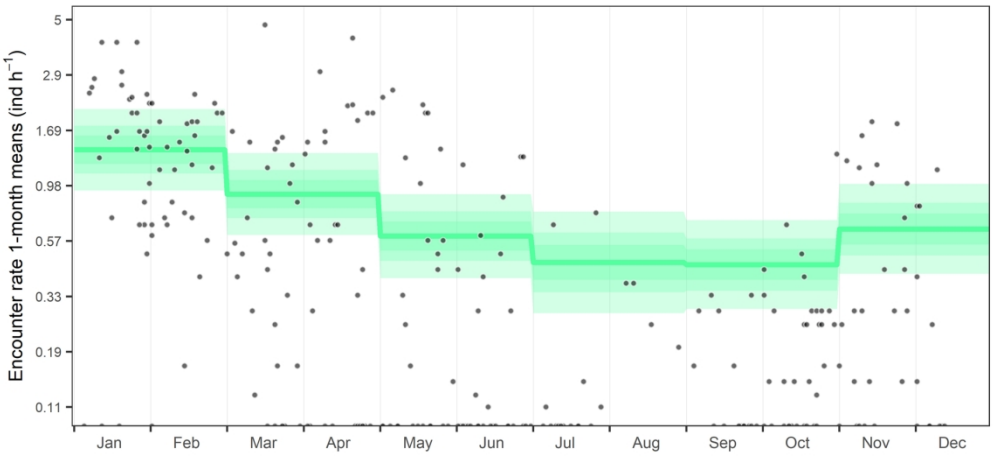

FIGURE 7 Partial seasonal effects of the bimester of the year on fin whale encounter rates. The green line corresponds to the median prediction and the green ribbons correspond to the 95%-, 75%-, and 50%-credible intervals, in incremental darkness.

169x78mm (300 x 300 DPI)

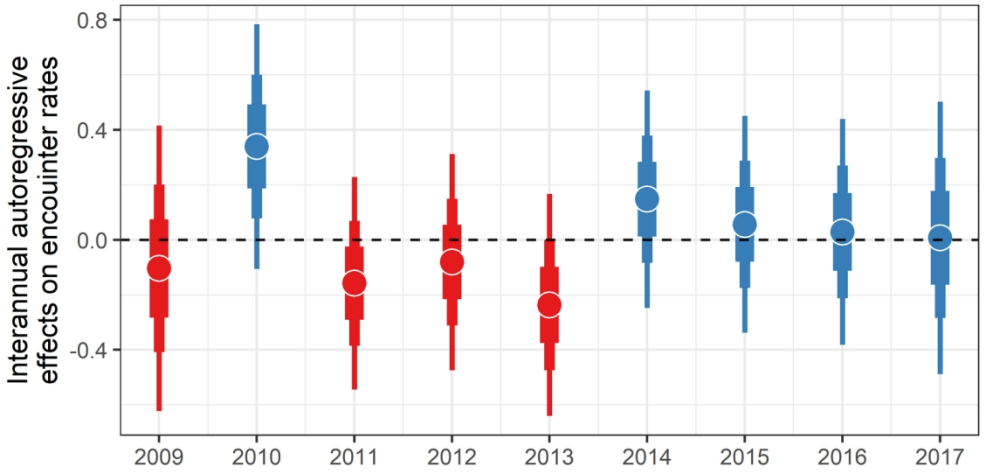

FIGURE 8. Interannual autoregressive effects on fin whale encounter rates (1-month running means), thus representing the interannual variations. Vertical bars show the median value only.

139x73mm (300 x 300 DPI)

TABLE 1. Fin type distribution for the Eastern Midriff Islands Region catalog. Total number of photo-identifications in the catalog was 559, with maximum two photos per individual (both sides of the dorsal fin). Total number of individuals in the catalog was 376. See Supporting Information 3 for fin type description.

Fin type	In catalog	%	No. with nicks	No. with scars	No. without nicks or scars
A	144	38.3	77	140	7
B	13	3.5	8	12	0
C	44	11.7	8	41	3
D	85	22.6	35	84	1
E	67	17.8	31	61	5
F	1	0.3	1	0	0
O	22	5.8	18	21	0

TABLE 2 m-*reduced matrix*, resulting from the integration of the information pertaining to both sides of the dorsal fin into one catalog, detailing the information contained in the fin whale capture histories for the present study. *i,j* = years; *R(i)* = individuals observed; *m(i,j)* = individuals observed during *i* that were first recaptured during *j*; *r(i)* = recaptures in *i*; and *m(j)* = recaptures in *j*.

Year (*i*)	*R(i)*	*m(i,j)*							*r(i)*
		2010-2011	2011-2012	2012-2013	2013-2014	2014-2015	2015-2016	2016-2017	
2009-2010	81	17	5	7	9	4	4	0	46
2010-2011	41		9	5	9	2	1	0	26
2011-2012	27			6	12	4	0	0	22
2012-2013	23				16	1	0	0	17
2013-2014	85					31	8	3	42
2014-2015	58						29	1	30
2015-2016	43							0	0
m(j)		17	14	18	46	42	42	4	

TABLE 3 Goodness-of-fit test results for the Cormack-Jolly-Seber model per subcomponent. TEST2.CT checks for trap dependence. The transient subcomponent 3.SR is shown per year. The only statistically significant *p*-value is highlighted in bold.

Test	Component	χ^2	*df*	*p-value*
General	TEST2.CT	9.71	5	0.084
General	TEST2.CL	2.865	6	0.826
General	TEST3.Sm	3.58	6	0.734
General	TEST3.Sr	9.65	5	0.086
3.Sr Sub C.	2011-2012	0.644	1	0.422
3.Sr Sub C.	2012-2013	0.345	1	0.557
3.Sr Sub C.	2013-2014	0.313	1	0.576
3.Sr Sub C.	2014-2015	2.028	1	0.154
3.Sr Sub C.	2015-2016	6.320	1	**0.012***
3.Sr Sub C.	2016-2017	0	0	0

TABLE 4 Jolly-Seber POPAN models, descriptive statistics, and $QAIC_c$ support for model selection. Parameters: ϕ = survival probability; p = capture probability; *pent* = entry probability; and N= abundance estimate. A dot in parentheses (.) indicates that the parameter is constant for all occasions, while (*time*) indicates time dependence, corresponding to a different parameter value for each occasion, (*T*) indicates a temporal linear trend.

Rank	Model	Parameters	$QAIC_c$	$\Delta QAIC_c$	$QAIC_c$ weight	QDeviance
I	$\phi_{(trans:Time)}p_{(time)}pent_{(time)}N_{(}$	15	734.41	0	0.27272	703.0262
II	$\phi_{(trans)}p_{(time)}pent_{(time)}N_{(.)}$	15	734.81	0.4053	0.2227	703.4314
III	$\phi_{(trans+Time)}p_{(time)}pent_{(time)}N$	16	735.88	1.4679	0.13091	702.3051
IV	$\phi_{(trans)}p_{(time)}pent_{(T)}N_{(.)}$	13	736.96	2.5482	0.07628	709.9148
V	$\phi_{(trans:Time)}p_{(time)}pent_{(.)}N_{(.)}$	12	737.00	2.5944	0.07453	712.1125
VI	$\phi_{(trans:Time)}p_{(time)}pent_{(T)}N_{(.)}$	13	737.05	2.6419	0.07279	710.0084
VII	$\phi_{(trans)}p_{(time)}pent_{(.)}N_{(.)}$	12	737.05	2.6438	0.07272	712.1619
VII	$\phi_{(trans+Time)}p_{(time)}pent_{(Time)}N$	14	738.26	3.8515	0.03975	709.0541
VIII	$\phi_{(trans+Time)}p_{(time)}pent_{(.)}N_{(.)}$	13	738.37	3.9627	0.0376	711.3292

TABLE 5 Jolly-Seber POPAN model averaged annual abundance estimates, inflated with the mark ratio (*MR=0.48*). Unconditional standard error, which considers model selection uncertainty. The last column is the percentage of variation due to model differences in model averaging.

Year	Abundance	SE_{Un}	Lower 95% CL	Upper 95% CL	%variation MS
2010-2011	313	41.65	232	395	32.61%
2011-2012	284	36.39	213	366	39.71%
2012-2013	256	40.30	177	338	56.88%
2013-2014	276	30.09	217	357	20.48%
2014-2015	242	34.38	175	324	37.20%
2015-2016	211	43.29	126	293	42.72%

TABLE 6 Cormack-Jolly-Seber models with descriptive statistics ranked by QAICc. The *a2* notation separates the parameter of survival for the first time an individual whale was sighted from the parameter for whales seen multiple times.

Rank	Model	#par	$QAIC_c$	$\Delta QAIC_c$	Weight	QDeviance
I	$\phi_{(a2-./.)}p_{(t)}$	9	688.8398	0	0.93337	106.4257
II	$\phi_{(a2-./t)}p_{(t)}$	14	696.1809	7.3411	0.02377	103.0596
III	$\phi_{(t)}p_{(t)}$	13	696.4583	7.6185	0.02069	105.5033
IV	$\phi_{(a2-./.)}p_{(a2-t/t)}$	15	697.4073	8.5675	0.01287	102.107
V	$\phi_{(a2-t/.)}p_{(t)}$	15	698.3168	9.477	0.00817	103.0165
VI	$\phi_{(a2-t/t)}p_{(t)}$	19	702.2541	13.4143	0.00114	98.1088

TABLE 7. Probability of recapture obtained from the top- ranked CJS model. Estimates are not shown for the first or last sampling periods because they are unreliable.

Year	*p*	SE	Lower 95% CL	Upper 95% CL
2011	0.31	0.07	0.19	0.46
2012	0.21	0.06	0.12	0.34
2013	0.25	0.06	0.16	0.37
2014	0.66	0.07	0.51	0.78
2015	0.48	0.07	0.35	0.61
2016	0.46	0.07	0.33	0.60

Table S1 Search effort (surveys by year and hours by year and season) and sightings in the Eastern Midriff Islands Region, 2009-2017. TCW=Transition cold-warm season, and TWC= Transition warm-cold season.

	2009-2010	2010-2011	2011-2012	2012-2013	2013-2014	2014-2015	2015-2016	2016-2017	Total
Surveys	40	35	33	38	41	35	35	30	287
Cold (h)	88	103	144	104	170	169	137	99	1012
TCW (h)	41	28	19	51	26	12	42	20	239
Warm (h)	72	71	66	7	49	71	48	39	492
TWC (h)	26	22	13	38	29	8	17	29	182
Total (h)	227	223	241	269	274	259	244	187	1924
Sightings	89	31	34	28	128	68	67	10	454

Supporting Information 2

Photo-quality grading criteria used in this work. It was based on the system used by the Sarasota Dolphin Research Program curated by Kim Urian, which derived the measures from Friday et al. (2000).

Photograph quality:

Based on the quality of the photograph, independent of the distinctiveness of the fin.

The overall score is based on an evaluation and sum of the following characteristics (these scores are absolute values, not a sliding scale)

- Focus/Clarity

Crispness or sharpness of the image. Lack of clarity may be caused by poor focus, excessive enlargement, poor development or motion blur; for digital images, poor resolution resulting in large pixels.

2 = excellent focus; 4 = moderate focus; 9 = poor focus, very blurry

- Contrast

Range of tones in the image. Images may display too much contrast or too little. Photographs with too much contrast lose detail as small features wash out to white. Images with too little contrast lose the fin into the background and features lack definition.

1 = ideal contrast ; 3= either excessive contrast or minimal contrast

• Angle

Angle of the fin to the camera.

1 = perpendicular to camera 2 = slight angle 8 = oblique angle

•Partial

A partial rating is given if so little of the fin is visible that the likelihood of re-identifying the individual is compromised on that basis alone. Fins obscured by waves, *Xenobalanus*, or other whales, would be evaluated using this rating.

1 = the fin is fully visible, leading & trailing edge 8= the fin is partially obscured

•Proportion of the frame filled by the fin

An estimate of the percentage area the fin occupies relative to the total area of the frame.

1 = greater than 5%; subtle features are visible 5 = less than 1%; fin is very distant

To score *Overall Photographic Quality*, the scores for each characteristic are summed:

Q1: 6 - 9: Excellent quality

Q2: 10–12: Average quality

Q3: >12 : Poor quality

References:

Friday, N., Smith, T.D., Stevick ,P.T., Allen, J. (2000) Measurement of photographic quality and individual distinctiveness for the photographic identification of humpback whales, *Megaptera novaeangliae*. Marine Mammal Science, 16(2), 355-374. https://doi.org/10.1111/j.1748-7692.2000.tb00930.x

Sarasota Dolphin Research Program. (2005) Field Techniques and Photo-Identification Handbook. Chicago Zoological Socierty and Dolphin Biology Rearch Institute c/o Mote Marine Laboratory. Sarasota, Florida, USA.

Supporting Information 3

Fin features used to grade distinctiveness

Table S3.1 Fin type shape descriptions (Agler et al., 1990).

Type	Description
A	Large and broad
B	Long, thin and pointed
C	Small and triangular, trailing edge straight or perpendicular to the body
D	The leading edge was bent posteriorly and/or the fin was very hooked
E	Short low versions of type A
F	All have humps on the back of the whale anterior to the insertion of the dorsal fin
O	All remaining fins – including whales with no fins or fins that were difficult to categorize

Table S3.2 Scar type descriptions (Agler et al., 1990).

Code	Type	Description
L	Linear	Lines less than two inches wide
S	Scrape	Line markings greater than 2 inches wide
C	Circular	Round or circular shapes of any size
D	Dent	Any depression
T	Tracks	Linear scar intersected by perpendicular lines – probably caused by a small boat propeller.
B	Braid	Large propeler scars that appear raised and often braided
P	Piece missing	Piece or chunk missing from the body, usually the caudal peduncle
A	Attachment	Usually a parasitic copepod, lamprey, etc.

Reference:

Agler, B.A., Beard, J.A., Bowman, R.S., Corbett, H.D., Frohock, S.E., Hawvermale, M.P., Katona, S.K., Sadove, S.S., & Seipt, I.E. (1990). Fin whale (*Balaenoptera physalus*) photographic identification: methodology and preliminary results from the western north Atlantic. *Reports of the International Whaling Commission (Special Issue 12)*, 349-356.